



Statistical Properties of the Acoustic Field in Inhomogeneous Oceanic Environments

Oleg A. Godin^{1, 2} and Alexander G. Voronovich²

¹CIRES, University of Colorado at Boulder

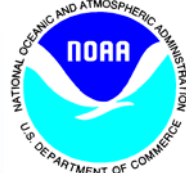
² NOAA/Environmental Technology Laboratory



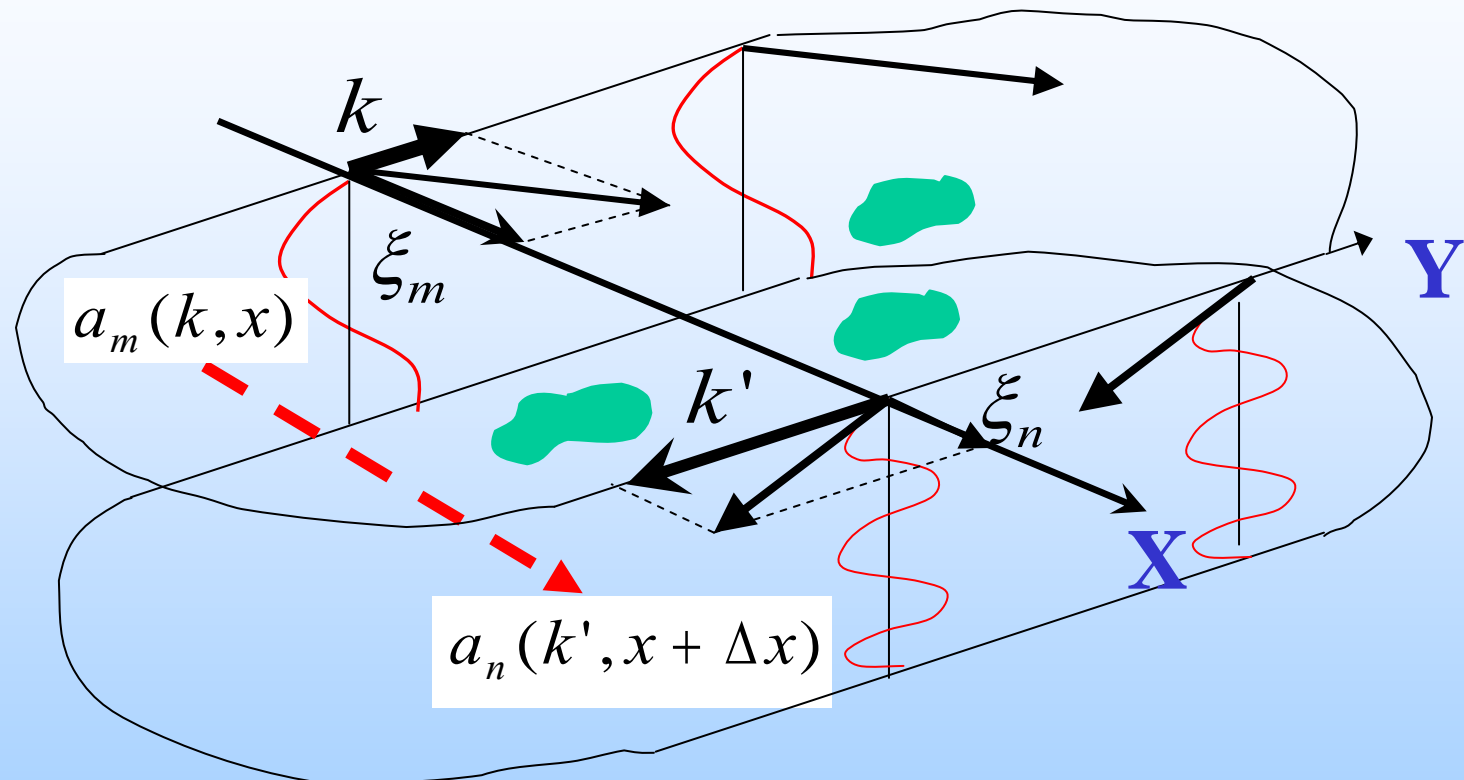
Outline



1. Scattering matrix for acoustic modes
 - 1.1 Application to uneven bottom effects
 - 1.2 Application to scattering from internal wave soliton
2. Hydrodynamic description of the IW solitons
3. Chernov – Markov approximation for propagation of low frequency acoustic fields in random waveguide
4. 3-D vs. 2-D acoustics for average acoustic field
5. Conclusions



Acoustic mode scattering matrix



$$p = u_m(z) \exp(i\xi_m x + iky) + \sum_n u_n(z) \int dk' S_{nm}(k', k) \exp[i\xi'_m(x - \Delta x) + ik'y]$$



Field transformation – SPM limit



$$a_n(k, x + \Delta x) = a_n(k, x) e^{i \xi_n \Delta x} + \sum_m \int dk' S_{nm}(k, k') a_m(k', x)$$

First order scattering :

$$S_{mn}(k', k) = \frac{i}{4\pi} \frac{\omega^2}{c_{00}^2} \frac{1}{\xi'_{m}} \int_0^{\Delta x} dx \int dy \exp \left[-i(\xi'_{m} - \xi_n)x - i(k - k')y \right].$$

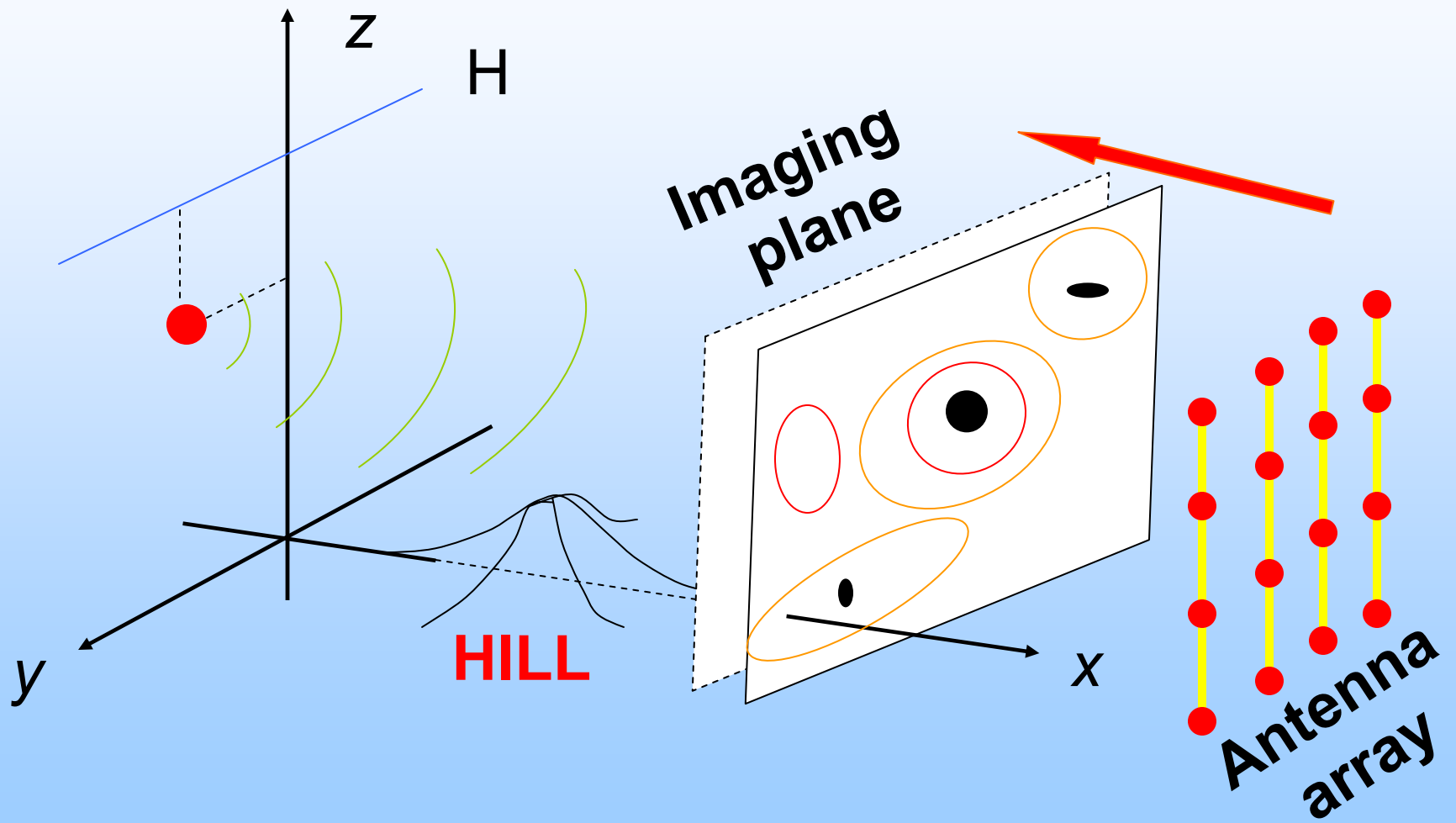
$$\cdot \int dz \Delta n^2(x, y, z) u_m(z) u_n(z)$$



1.1 Application to Uneven Bottom Effects

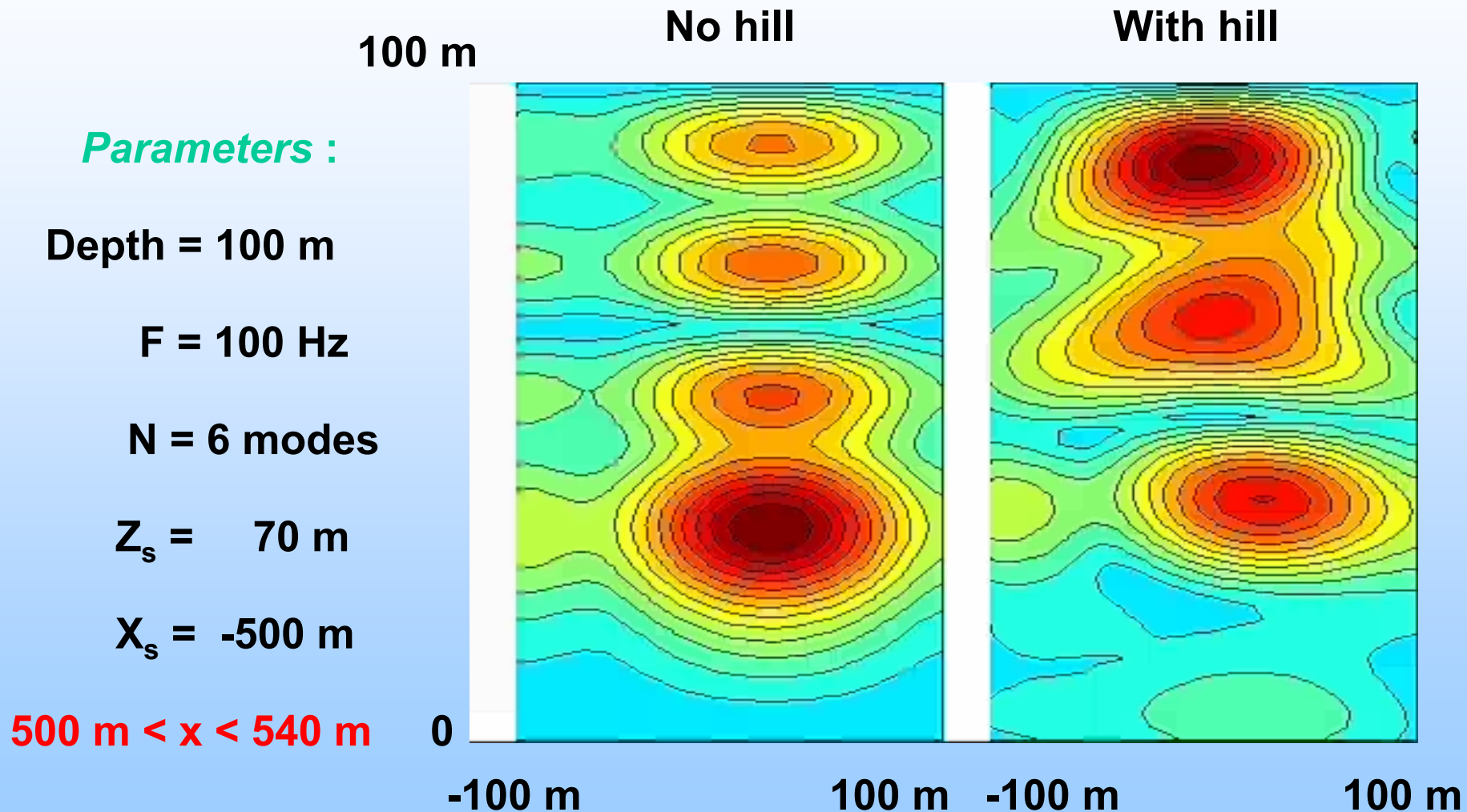


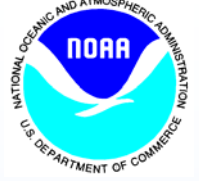
Source imaging: utilizing a concept of scattering matrix





Source image as a function of X

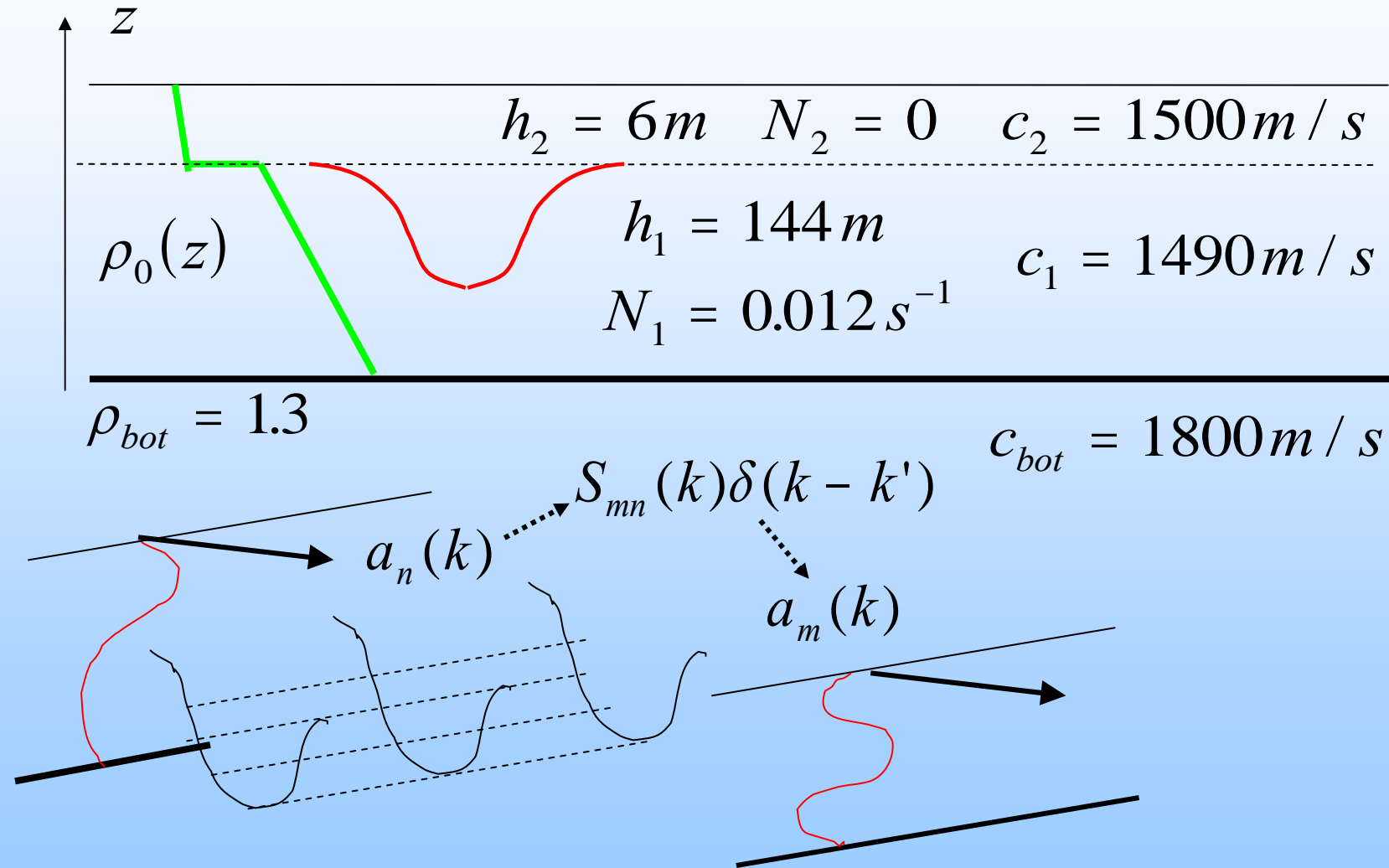


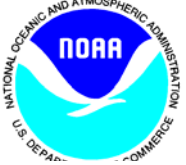


1.2 Application to Scattering from Internal Wave Soliton



Pekeris waveguide with strong IW soliton

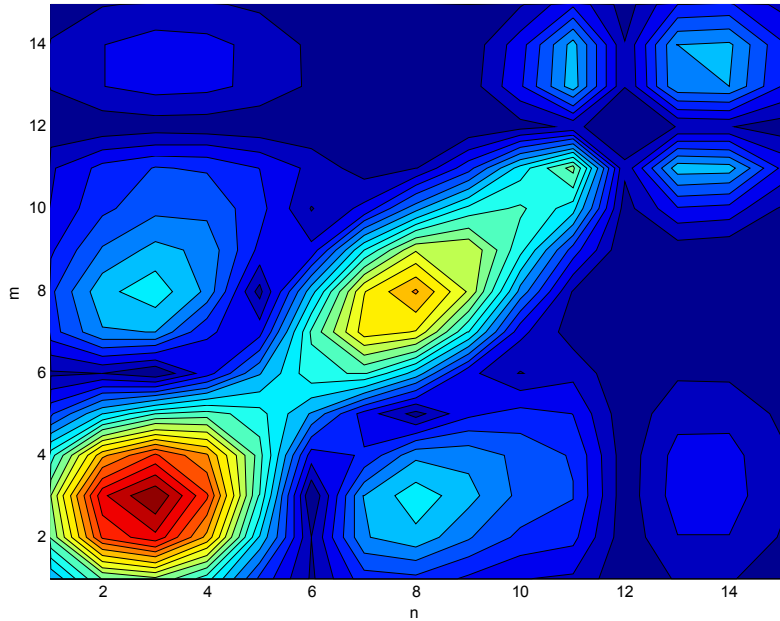




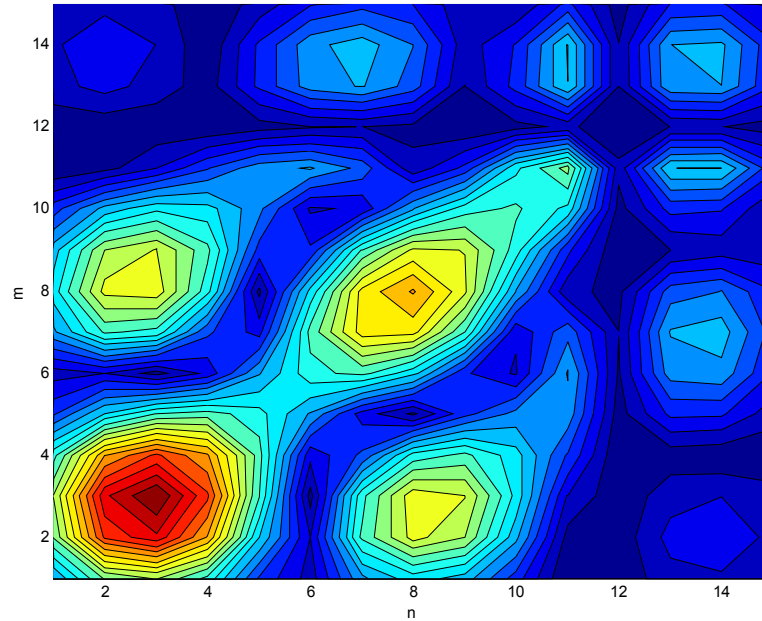
Scattering matrix at IW soliton: F=100 Hz, h=27.8 m; N=15 modes



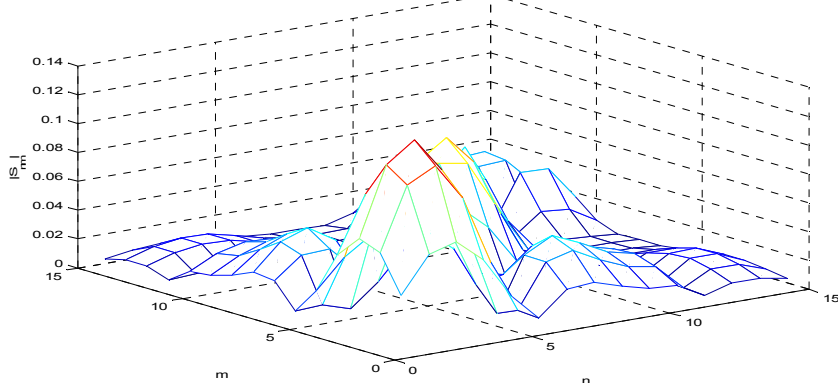
Mode Scattering Matrix at IW soliton: $h_0=27.8$ m, $F=100$ Hz, $\alpha=0$ deg



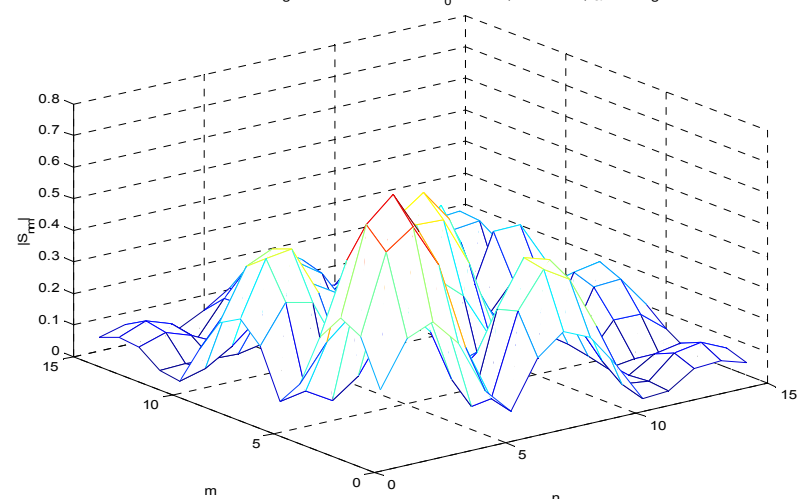
Mode Scattering Matrix at IW soliton: $h_0=27.8$ m, $F=100$ Hz, $\alpha=80$ deg



Mode Scattering Matrix at IW soliton: $h_0=27.8$ m, $F=100$ Hz, $\alpha=0$ deg



Mode Scattering Matrix at IW soliton: $h_0=27.8$ m, $F=100$ Hz, $\alpha=80$ deg



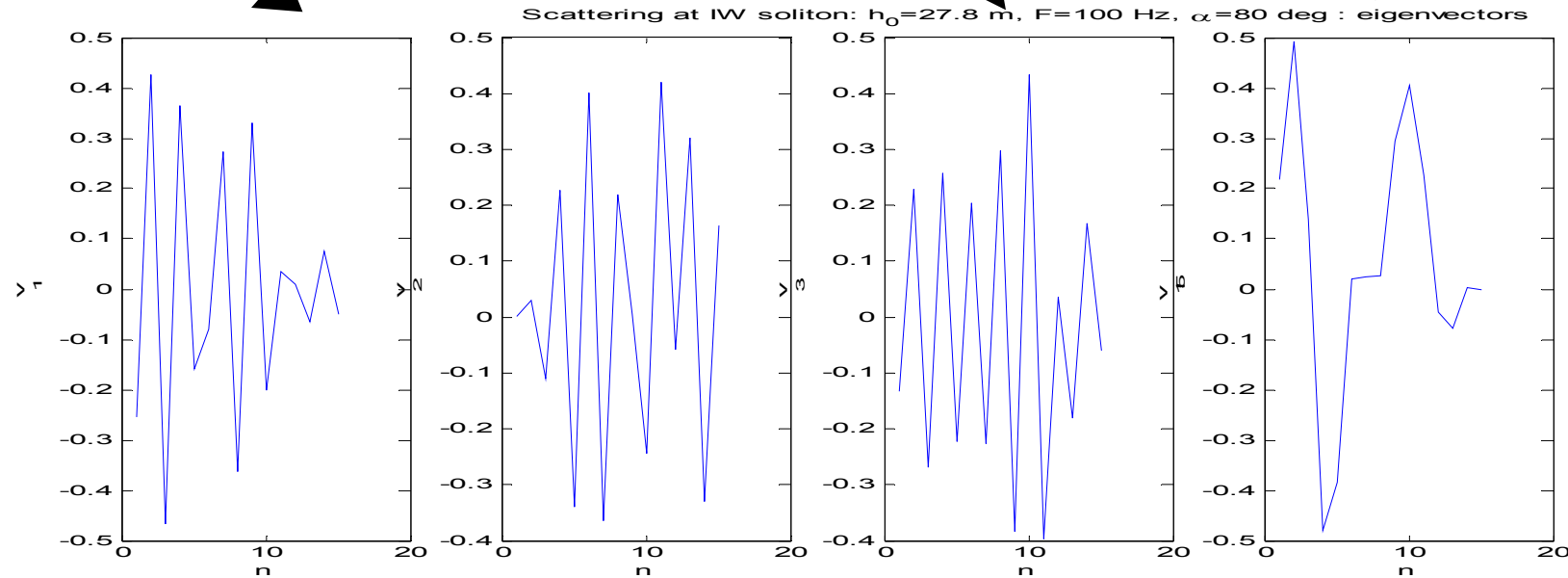
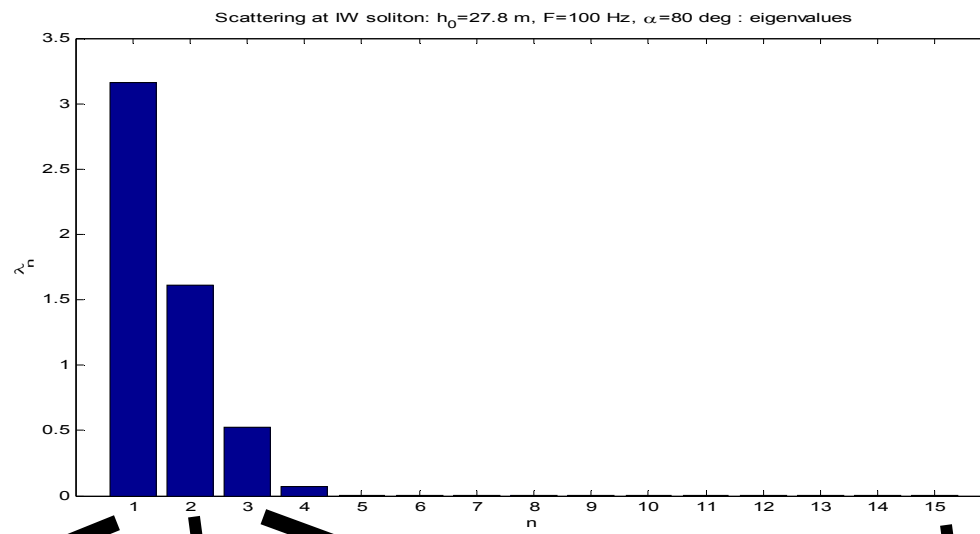


Spectrum of S-matrix and eigenvectors



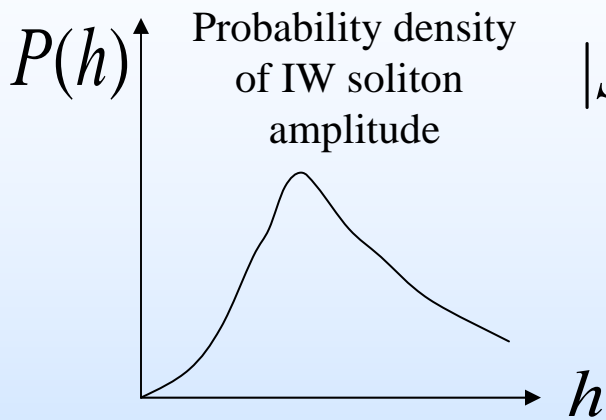
Strong
scattering
effects

Weak
scattering
effects

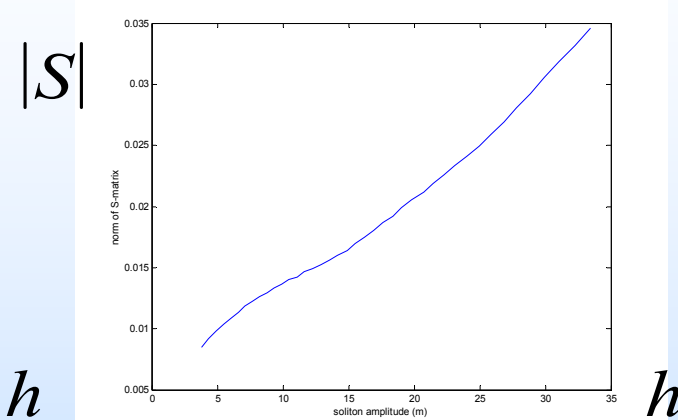




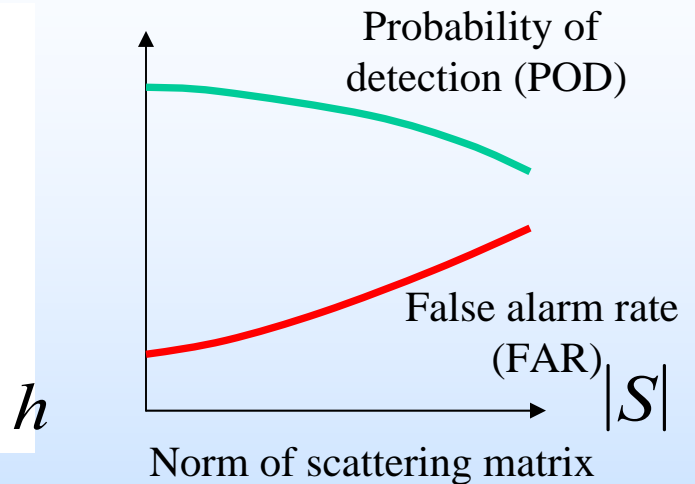
Uncertainty due to IW solitons



Hydrophysics



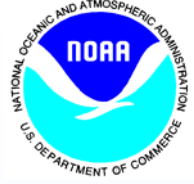
Propagation



Detection algorithm

$$\langle POD \rangle = \int POD(|S|(h)) \cdot P_{sol}(h) dh$$

$$\langle FAR \rangle = \int FAR(|S|(h)) \cdot P_{sol}(h) dh$$



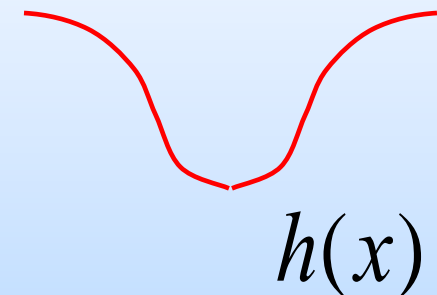
2. Hydrodynamic Description of the Internal Wave Solitons



Strong IW soliton for 2.5 layer model



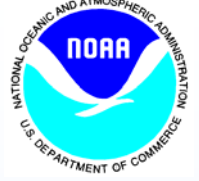
$$\Psi_{xx}^{(2)} + \Psi_{zz}^{(2)} + \frac{N_2^2}{c^2} \Psi^{(2)} = 0$$



$$\Psi_{xx}^{(1)} + \Psi_{zz}^{(1)} + \frac{N_1^2}{c^2} \Psi^{(1)} = 0$$

Governing equation:

$$-\frac{1}{2}(1+h_x^2)(c+\Psi_z^{(1)})^2 + \frac{1}{2}(1+h_x^2)(c+\Psi_z^{(2)})^2 - g\Delta\rho h = 0$$

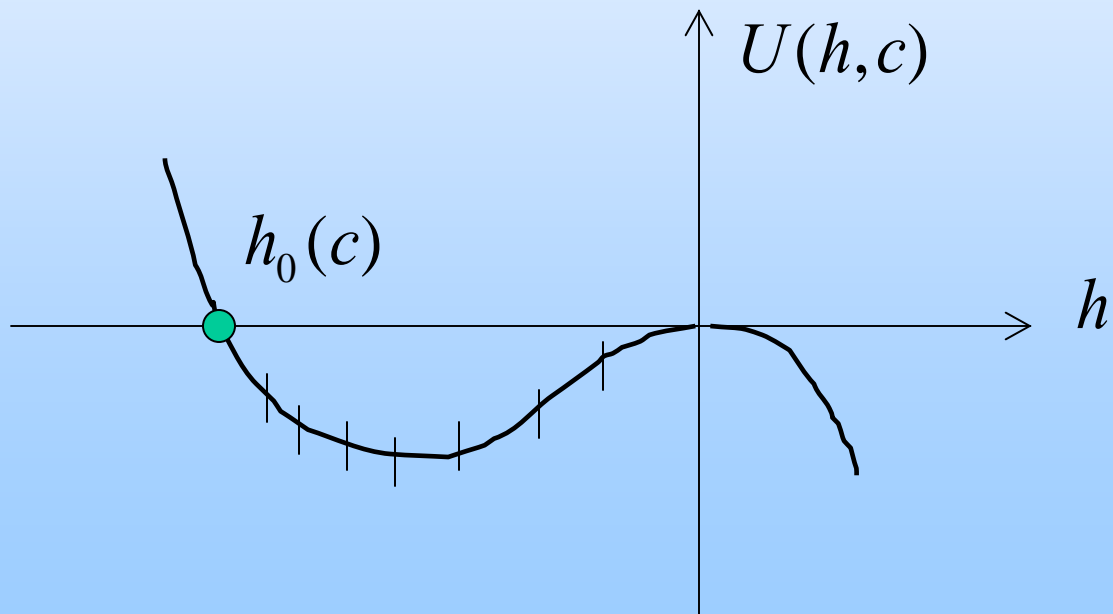


Strong IW solitons



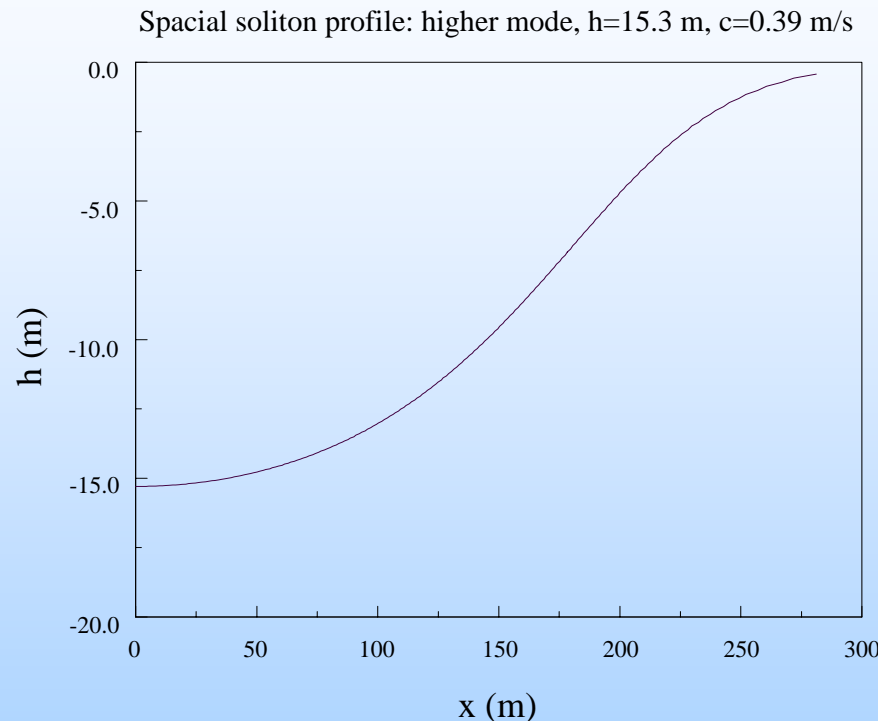
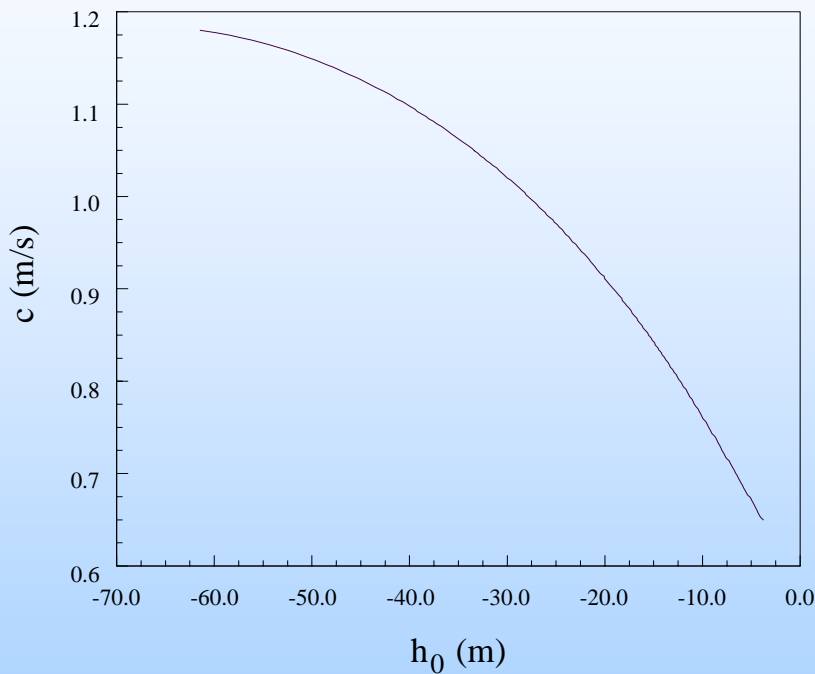
$$A(h)h_{xx} + B(h)h_x^2 + C(h) = 0$$

$$\frac{1}{2} \left(\frac{dh}{dx} \right)^2 + U(h) = 0$$





Soliton profile and speed vs. amplitude dependence



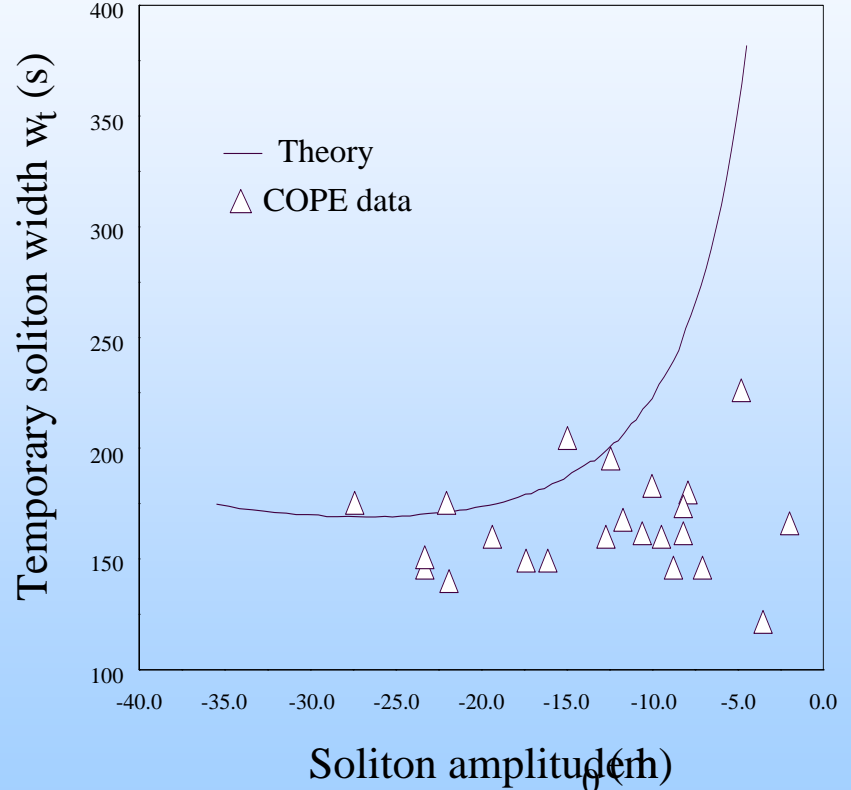
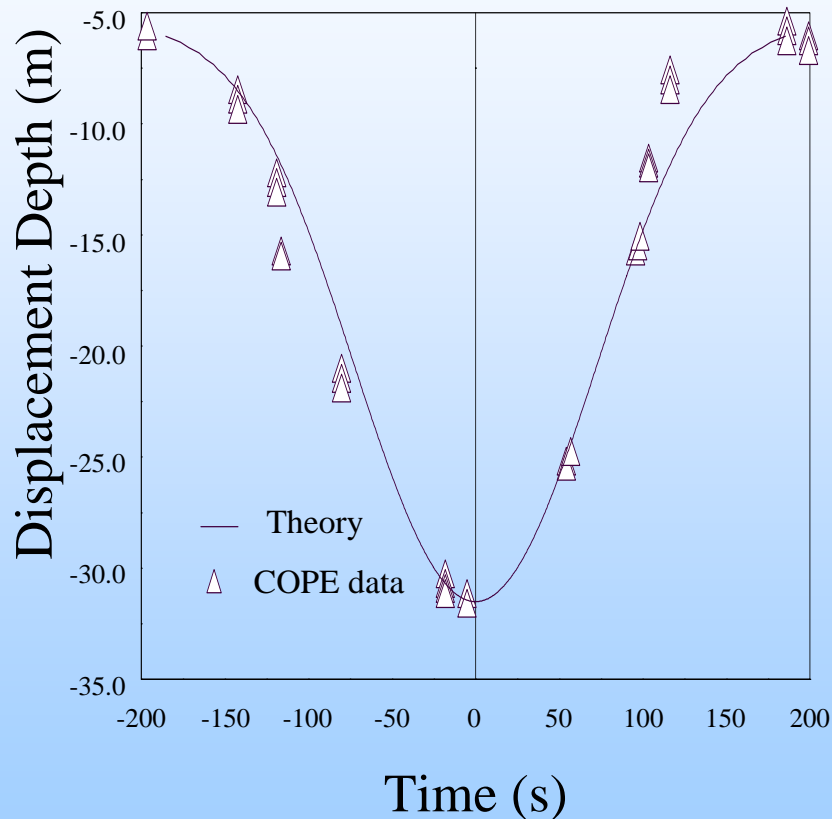
$$\frac{1}{2} \left(\frac{dh}{dx} \right)^2 + U(h, c) = 0$$



Comparison with COPE experiment



Internal solitary wave profile





3. Chernov – Markov approximation for propagation of low frequency acoustic fields in random waveguide



Modal scattering matrix



$$a_n(k, x + \Delta x) = a_n(k, x) e^{i \xi_n \Delta x} + \sum_m \int dk' S_{nm}(k, k') a_m(k', x)$$

$$\Psi(x, y, z) = \sum_n u_n(z) \int dk a_n(k, x) e^{i \xi_n x + iky}$$

Some notations:

$$\frac{d^2 u_n}{dz^2} + \left(\frac{\omega^2}{c^2(z)} - b_n^2 \right) u_n = 0, \quad u_n(0) = u_n(-\infty) = 0$$

$$\xi_n = \xi_n(k) = \sqrt{b_n^2 - k^2} \quad \int u_n u_m dz = \delta_{nm}$$



Statistical description



$$a_n(k, x) = \bar{a}_n(k, x) + \Delta a_n(k, x)$$

Characteristics
of the field
(to be calculated)

$$\langle \Delta a_n(k - \eta/2, x) \Delta a_m^*(k + \eta/2, x) \rangle = B(k, x; \eta)$$

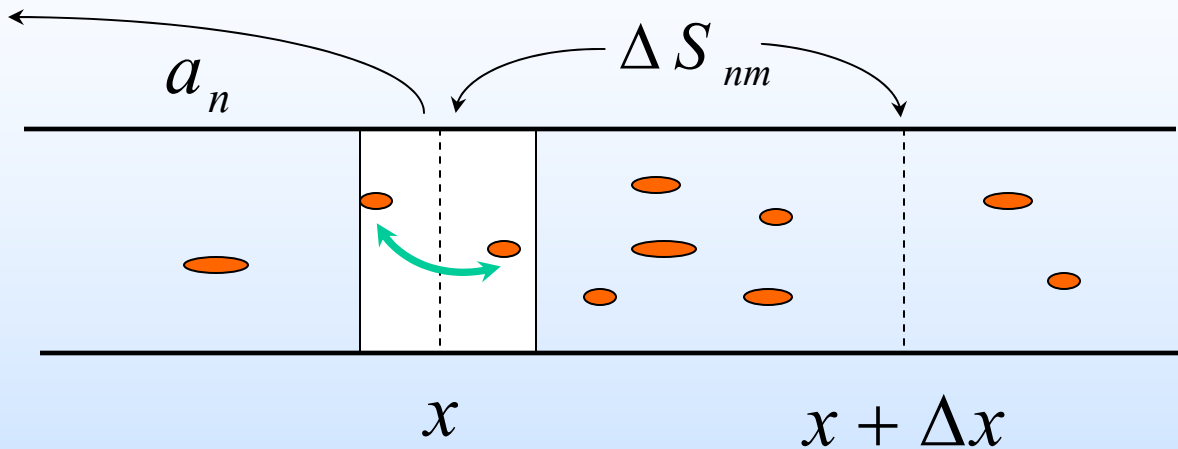
$$S_{mn}(k, k_0) = \Delta x \bar{S}_{mn}(k) \delta(k - k_0) + \Delta S_{mn}(k, k_0)$$

$$\begin{aligned} \langle \Delta S_{n_1 m_1}(k - \eta/2, k_0 - \eta/2) \Delta S_{n_2 m_2}^*(k + \eta/2, k_0 + \eta/2) \rangle &= \\ &= \Delta x E_{n_1 m_1, n_2 m_2}(k, k_0; \eta) \delta(\eta - \eta_0) \end{aligned}$$

Statistical parameters
of the medium



Chernov-Markov approximation



$$\langle a_n(k,x) \cdot \Delta S_{k_1 m_1} \cdot \Delta S^*_{k_2 m_2} \rangle = \langle a_n(k,x) \rangle \langle \Delta S_{k_1 m_1} \cdot \Delta S^*_{k_2 m_2} \rangle$$

$$\langle \Delta a_n \cdot \Delta a_m \cdot S_{kl} \rangle = \langle \Delta a_n \cdot \Delta a_m \rangle \langle S_{kl} \rangle$$

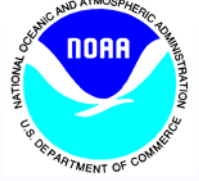
etc.



Governing equations for correlations



$$\begin{aligned} B_{nn'}(k, x + \Delta x; \eta) &= B_{nn'}(k, x; \eta) e^{i[\xi_n(k - \eta/2) - \xi_{n'}(k + \eta/2)]\Delta x} + \\ &+ \Delta x \sum_{m'} e^{i\xi_n(k - \eta/2)\Delta x} \bar{S}_{n'm'}^*(k + \eta/2) B_{nm'}(k, x; \eta) + \\ &+ \Delta x \sum_{m'} e^{-i\xi_{n'}(k + \eta/2)\Delta x} \bar{S}_{nm}(k - \eta/2) B_{mn'}(k, x; \eta) + \\ &+ \Delta x \sum_{m, m'} \int dk' E_{nn', mm'}(k, k'; \eta) B_{mm'}(k', x; \eta) + \\ &+ \Delta x \sum_{m, m'} \int dk' E_{nn', mm'}(k, k'; \eta) \bar{a}_m(k' - \eta/2, x) \bar{a}_{m'}^*(k' + \eta/2, x) + \\ &+ \Delta x \sum_{m, m'} \bar{S}_{nm}(k - \eta/2) \bar{S}_{n'm'}^*(k + \eta/2) B_{mm'}(k', x; \eta) \end{aligned}$$



Optical theorem



$$\begin{aligned} & \xi_{n_1} e^{i\xi_{n_1} \Delta x} \bar{S}_{n_1 n_2}^*(k) + \xi_{n_2} e^{-i\xi_{n_2} \Delta x} \bar{S}_{n_2 n_1}(k) + \\ & + \sum_m \int dk' \xi_m E_{mm, n_1 n_2}(k', k; 0) + \Delta x \sum_m \xi_m \bar{S}_{mn_1}(k) \bar{S}_{mn_2}^*(k) = 0 \end{aligned}$$



Calculation of scattering



$$\Psi(\vec{r}, z) = \Psi_{in}(\vec{r}, z) - \frac{\omega^2}{c_{00}^2} \int \theta(x - x') G_0(\vec{r} - \vec{r}'; z, z') \Delta n^2(\vec{r}', z') \Psi(\vec{r}', z') d\vec{r}' dz'$$

Index of refraction fluctuations

Forward scattering approximation

$$G_0(\vec{r}; z, z') = -\frac{i}{4\pi} \sum_m u_m(z) u_m(z') \int \frac{dk}{\xi_m(k)} \exp[i\xi_m(k)x + ikz']$$



Scattering cross section



$$\sigma_{nm}(k) = e_{nn,mm}(k) = \frac{\pi}{2} \left(\frac{\omega}{c_{00}} \right)^4 \sum_a P_a(b_n - b_m, k) \left[N_{nm}^a \left(\sqrt{(b_n - b_m)^2 + k^2} \right) \right]^2$$

↑ ↑
Spectrum of fluctuations *Acoustic-IW modes interaction matrix*

Optical theorem:

$$2 \operatorname{Re} s_{nn} + \sum_m \frac{1}{b_m} \int dk \sigma_{nm}(k) = 0$$



Diffusion approximation



$$\begin{aligned}\frac{\partial \tilde{I}_n}{\partial x} = & -\beta_n \tilde{I}_n + \sum_m \sigma_{nm}^{(0)} \tilde{I}_m + \sum_m \sigma_{nm}^{(2)} \frac{\partial^2 \tilde{I}_m}{\partial k^2} + \\ & + \sum_m \sigma_{nm}^{(0)} b_m |\bar{a}_m(0, x)|^2 e^{-2\beta_m x}\end{aligned}$$

$$\tilde{I}_n = b_n I_n(k, x; \eta)$$

$$\sigma_{nm}^{(0)} = \frac{1}{b_n b_m} \int dk \sigma_{nm}(k) \quad , \quad \sigma_{nm}^{(2)} = \frac{1}{b_n b_m} \int dk \sigma_{nm}(k) k^2$$



Solution at large X



$$\tilde{I}_n(k, x) \rightarrow \sqrt{\frac{\pi}{k_0^4 l_* x}} \exp\left(-\frac{k^2}{4k_0^4 l_* x}\right)$$

Angular spectrum:

$$\frac{\delta k}{k_0} = k_0 \sqrt{l_* x}$$

Correlation function:

$$C_n(x, \Delta y) = \frac{1}{b_n} \int dk e^{ik\Delta y} \tilde{I}_n(k) = \frac{2\pi}{b_n} \exp\left[-k_0^4 l_* x (\Delta y)^2\right]$$



Numerical estimate



$$l_* = \frac{\pi}{2} \sum_{n,m,a} \int k^2 P_a(b_n - b_m, k) \left[N_{nm}^a \left(\sqrt{(b_n - b_m)^2 + k^2} \right) \right]^2 dk$$

For GM spectrum:

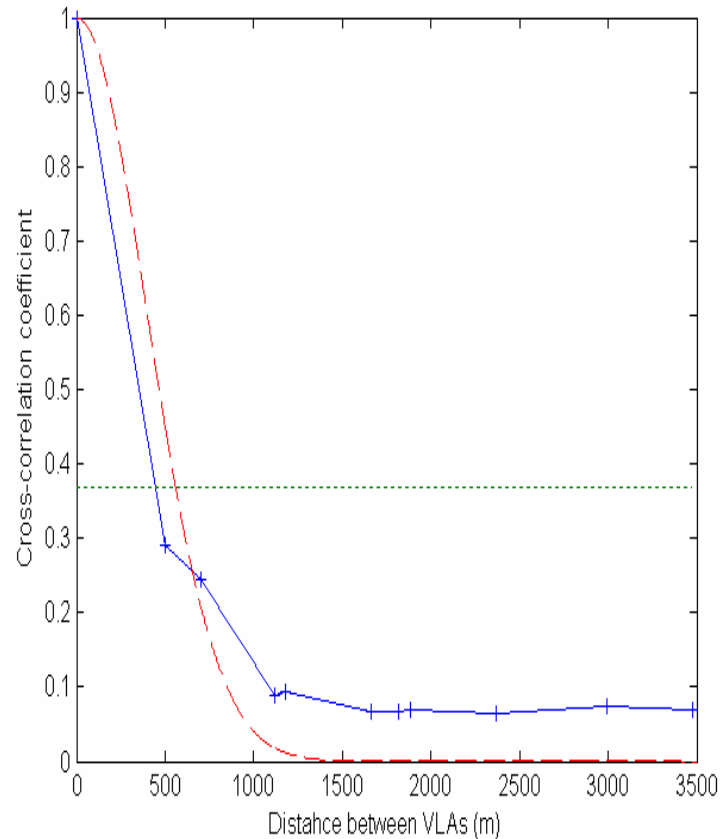
$$l_* = 5.4 \cdot 10^{-11} \text{ m}$$

$$\sigma_\alpha = \frac{\delta k}{k_0} = k_0 \sqrt{l_* x} = 4.6 \cdot 10^{-3} \approx 0.26^\circ$$

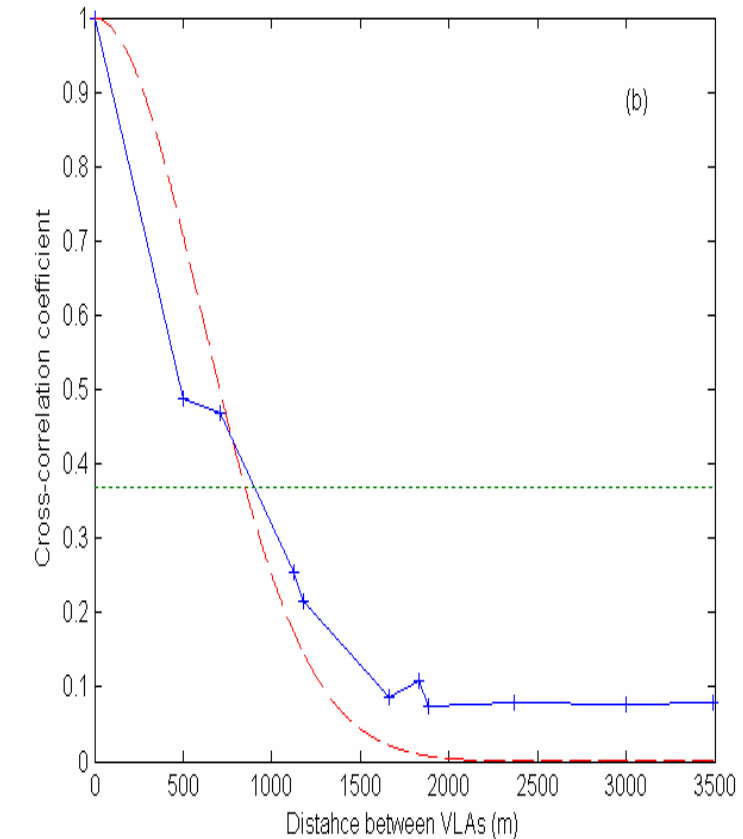
$$\rho_c = \frac{1}{k_0^2 \sqrt{l_* x}} \approx 700 \text{ m}$$



Cross-range correlation functions



$$r_c = 560 \text{ m}$$



$$r_c = 850 \text{ m}$$



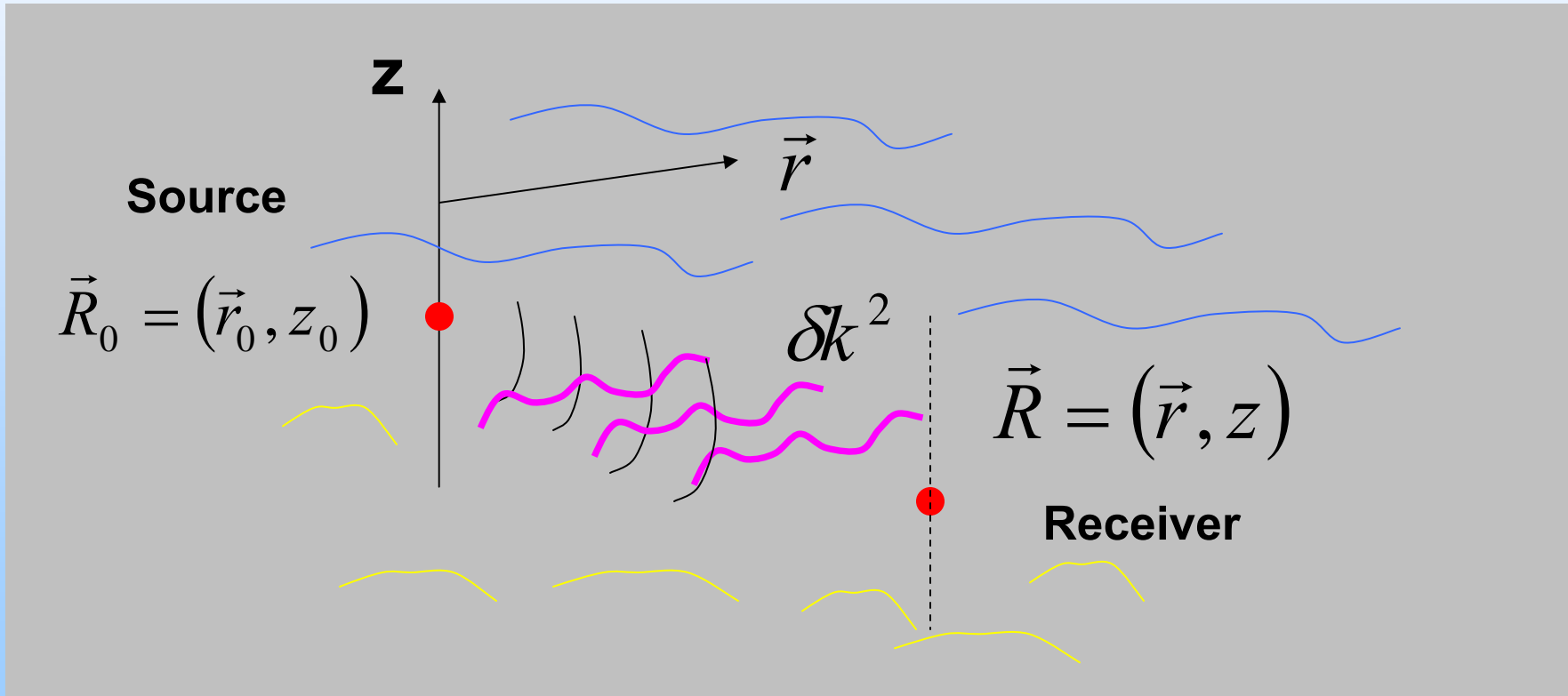
4. 3-D vs. 2-D acoustics for average acoustic field

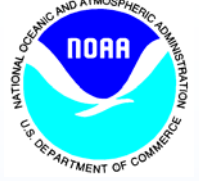


Problem formulation



$$\left(\frac{\partial^2}{\partial z^2} + \nabla^2 + k_0^2(z) - \delta k^2 \right) G(\vec{R}, \vec{R}_0) = \delta(\vec{r} - \vec{r}_0) \delta(z - z_0)$$





Governing equations



Helmholtz equation in the integral form:

$$G(\vec{R}, \vec{R}_0) = G_0(\vec{R}, \vec{R}_0) + \int G_0(\vec{R}, \vec{R}') \delta k^2(\vec{R}') G(\vec{R}', \vec{R}_0) d\vec{R}'$$

Green function of the unperturbed problem:

$$G_0(\vec{R}, \vec{R}_0) = G_0(\vec{r} - \vec{r}_0; z_0, z) = -\frac{i}{4} \sum_n u_n(z) u_n(z_0) H_0^{(1)}(\xi_n |\vec{r} - \vec{r}_0|)$$

Modes: $\left(\frac{d^2}{dz^2} + k_0^2(z) - \xi_n^2 \right) u_n = 0 \quad , \quad u_n(0) = u_n(-\infty) = 0$

Normalization: $\int_{-\infty}^0 u_n u_m dz = \delta_{nm}$



Average field calculation



Helmholtz equation in the operator notations:

$$G = G_0 + \hat{G}_0 \varepsilon G \quad , \quad \varepsilon = \delta k^2$$

Formal solution:

$$G = G_0 + \hat{G}_0 \varepsilon G_0 + \hat{G}_0 \varepsilon \hat{G}_0 \varepsilon G_0 + \dots$$

After averaging and summing up irreducible terms:

$$\bar{G} = G_0 + \hat{G}_0 \hat{\Sigma} G_0 + \hat{G}_0 \hat{\Sigma} \hat{G}_0 \hat{\Sigma} G_0 + \dots$$



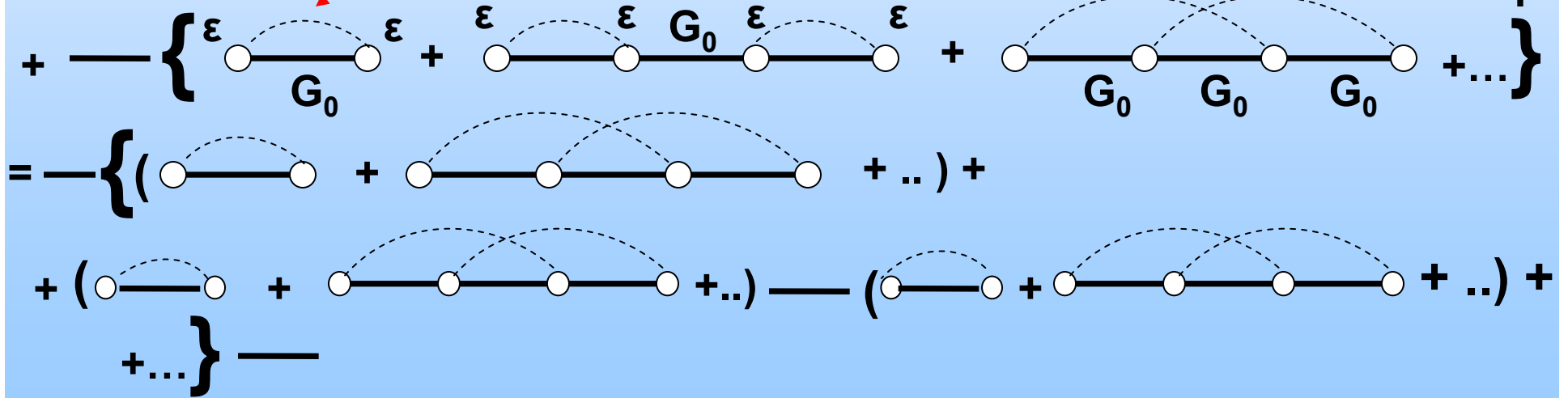
Average field calculation – cont.



$$\Sigma(\vec{R}, \vec{R}') = \left\langle \varepsilon(\vec{R}) G_0(\vec{R}, \vec{R}') \varepsilon(\vec{R}') \right\rangle + \\ + \int d\vec{R}_1 d\vec{R}_2 \left\langle \varepsilon(\vec{R}) G_0(\vec{R}, \vec{R}_1) \varepsilon(\vec{R}_2) \right\rangle G_0(\vec{R}_1, \vec{R}_2) \left\langle \varepsilon(\vec{R}_1) G_0(\vec{R}_2, \vec{R}') \varepsilon(\vec{R}') \right\rangle + ..$$

In diagrammatic notations:

$$\overline{G} = \text{---} +$$





An equation for average field



$$\overline{G} = G_0 + \hat{G}_0 \hat{\Sigma} G_0 + \hat{G}_0 \hat{\Sigma} \hat{G}_0 \hat{\Sigma} G_0 + \dots$$

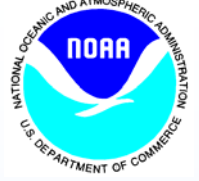
Applying Helmholtz operator:

$$\left(\frac{\partial^2}{\partial z^2} + \nabla^2 + k_0^2(z) - \hat{\Sigma} \right) \overline{G}(\vec{R}, \vec{R}_0) = \delta(\vec{r} - \vec{r}_0) \delta(z - z_0)$$

Burret Approximation: $\Sigma_0(\vec{R}, \vec{R}') = \langle \varepsilon(\vec{R}) G_0(\vec{R}, \vec{R}') \varepsilon(\vec{R}') \rangle = \langle \varepsilon(\vec{R}) \varepsilon(\vec{R}') \rangle G_0(\vec{R}, \vec{R}')$

Correlation function of fluctuations:

$$\langle \varepsilon(\vec{R}) \varepsilon(\vec{R}') \rangle = \mu(\vec{r} - \vec{r}'; z, z')$$



Average field modes



$$\begin{aligned}\Sigma_0(\vec{R}, \vec{R}') &= -\frac{i}{4} \sum_n u_n(z) u_n(z') H_0^{(1)}(\xi_n |\vec{r} - \vec{r}'|) \mu(\vec{r} - \vec{r}'; z, z') = \\ &= \int T_{\vec{k}}(z, z') e^{i\vec{k}(\vec{r} - \vec{r}')} \frac{d\vec{k}}{(2\pi)^2}\end{aligned}$$

$$T_{\vec{k}}(z, z') = \int H_0^{(1)}(\xi_n r) \mu(\vec{r}; z, z') e^{-i\vec{k}\vec{r}} d\vec{r}$$

The equation for the average field after Fourier transform:

$$\left(\frac{d^2}{dz^2} + k_0^2(z) - k^2 \right) \overline{G}_{\vec{k}}(z, z_0) - \int_{-\infty}^0 T_{\vec{k}}(z, z') \overline{G}_{\vec{k}}(z', z_0) dz' = \delta(z - z_0)$$



Perturbative case



$$\begin{aligned}\Delta \xi_n^2 &= -\left\langle u_n \left| T_{\xi_n} \right| u_n \right\rangle = - \int_{-\infty}^0 dz dz' u_n(z) u_n(z') T_{\xi_n}(z, z') = \\ &= \frac{i\pi}{2} \sum_m \int_{-\infty}^0 dz dz' u_n(z) u_n(z') u_m(z) u_m(z') \int_0^\infty H_0^{(1)}(\xi_m r) \mu(\vec{r}; z, z') J_0(\xi_n r) r dr\end{aligned}$$

Spectral representation of the correlation function:

$$\mu(\vec{r}; z, z') = \sum_a \int_0^\infty P_a(k) J_0(kr) \Phi_a(k, z) \Phi_a(k, z') k dk$$

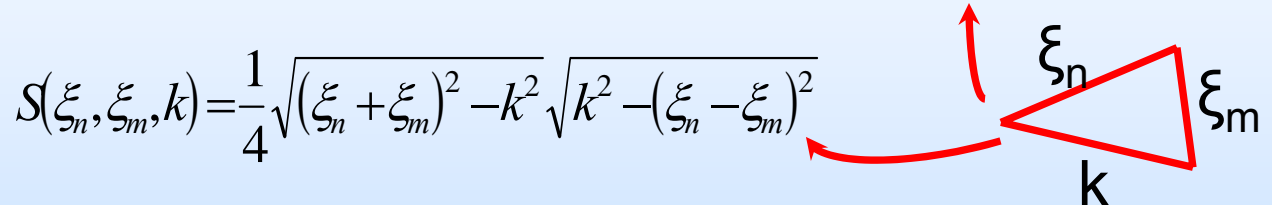
**For internal waves $\Phi_a(k, z)$ are internal wave mode profiles
and $P_a(k)$ is a modal spatial spectrum**



Average Green function



$$\text{Im} \Delta \xi_n^2 = \frac{1}{4} \sum_{m,a} \int_{|\xi_n - \xi_m|}^{\xi_n + \xi_m} P_a(k) \left[\int_{-\infty}^0 u_n(z) \Phi_a(k, z) u_m(z) dz \right]^2 \frac{k dk}{S(\xi_n, \xi_m, k)}$$



$$\bar{G}(\vec{R}, \vec{R}_0) = -\frac{i}{4} \sum_n u_n(z) u_n(z_0) H_0^{(1)}((\xi_n + \Delta \xi_n) |\vec{r} - \vec{r}_0|)$$

$$\bar{G}(\vec{R}, \vec{R}_0) \approx -\frac{i}{4} \sum_n u_n(z) u_n(z_0) H_0^{(1)}(\xi_n |\vec{r} - \vec{r}_0|) e^{-\text{Im} \Delta \xi_n |\vec{r} - \vec{r}_0|}$$



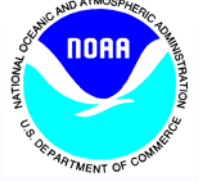
2D vs. 3D case



$$\left(\frac{\partial^2}{\partial z^2} + \frac{\partial^2}{\partial x^2} + k_0^2(z) - \delta k^2(x, z) \right) G = \delta(x - x_0) \delta(z - z_0)$$

$$G_0(x - x_0; z, z_0) = \sum_n u_n(z) u_n(z_0) \frac{\exp(\xi_n |x - x_0|)}{2i\xi_n}$$

$$\begin{aligned} \text{Im}\Delta\xi_n^2 &= \frac{1}{2} \sum_{m,a} \int_{|\xi_n - \xi_m|}^{\xi_n + \xi_m} P_a(k) \left[\int_{-\infty}^0 u_n(z) \Phi_a(k, z) u_m(z) dz \right]^2 \frac{k dk}{\xi_m \sqrt{k^2 - (\xi_n - \xi_m)^2}} + \\ &+ \frac{1}{2} \sum_{m,a} \int_{\xi_n + \xi_m}^{\infty} k dk P_a(k) \left[\int_{-\infty}^0 u_n(z) \Phi_a(k, z) u_m(z) dz \right]^2 \frac{1}{\xi_m} \left(\frac{1}{\sqrt{k^2 - (\xi_n - \xi_m)^2}} + \frac{1}{\sqrt{k^2 - (\xi_n + \xi_m)^2}} \right) \end{aligned}$$



2D vs. 3D – cont.



$$\text{Im} \Delta \xi_n^2 = \frac{1}{4} \sum_{m,a} \int_{|\xi_n - \xi_m|}^{\xi_n + \xi_m} P_a(k) \left[\int_{-\infty}^0 u_n(z) \Phi_a(k, z) u_m(z) dz \right]^2 \frac{\sqrt{(\xi_n + \xi_m)^2 - k^2}}{2\xi_m} \frac{k dk}{S(\xi_n, \xi_m, k)}$$

$$\frac{\sqrt{(\xi_n + \xi_m)^2 - k^2}}{2\xi_m} \approx \frac{\xi_n + \xi_m}{2\xi_m} = 1 + \frac{\xi_n - \xi_m}{2\xi_m}$$

$$\text{Im} \Delta \xi_n^2 = \frac{1}{4} \sum_{m,a} \int_{|\xi_n - \xi_m|}^{\xi_n + \xi_m} P_a(k) \left[\int_{-\infty}^0 u_n(z) \Phi_a(k, z) u_m(z) dz \right]^2 \frac{k dk}{S(\xi_n, \xi_m, k)}$$



Internal wave case

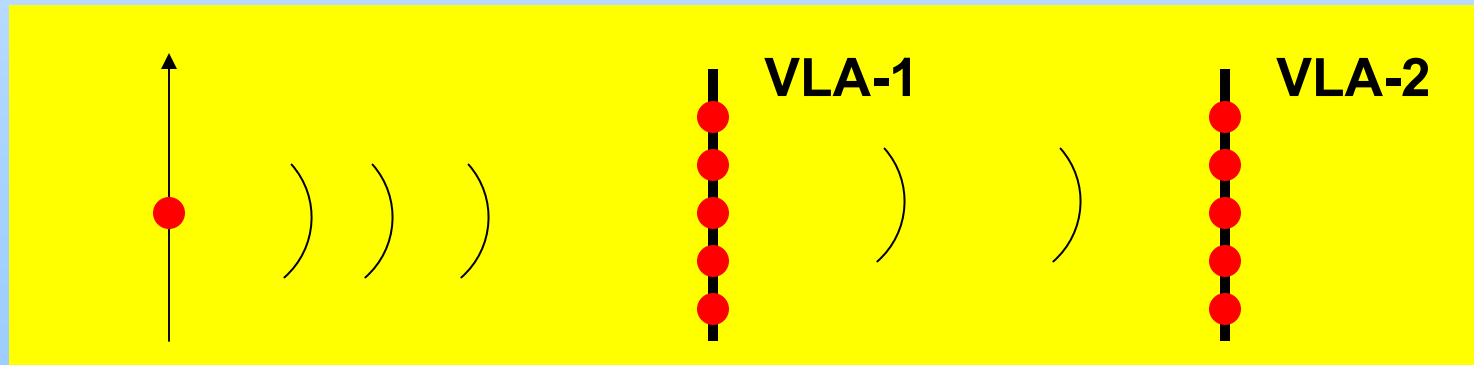


$$\text{Im } \Delta \xi_n^2 = \frac{1}{4} \sum_{m,a} \int_{|\xi_n - \xi_m|}^{\xi_n + \xi_m} P_a(k) \left[\int_{-\infty}^0 u_n(z) \Phi_a(k, z) u_m(z) dz \right]^2 \frac{k dk}{S(\xi_n, \xi_m, k)}$$

GM spectrum:

$$P_n(k) = \left(\frac{1}{c_0} \frac{dc_0}{dz} \right)^2 \times E_0 \frac{2k_* n_*}{\pi^3} \frac{n}{n^2 + n_*^2} \frac{k}{[k^2 + (k_* n)^2]^2} , \quad k_* = \frac{\pi}{B} \frac{\omega_i}{n_0}$$

Outline of the experimental scheme:





Conclusions



- The concept of Modal Scattering Matrix is useful for source imaging applications
- A hydrodynamic theory was developed for hydrodynamic description of the strongly non-linear internal wave solitons in the realistic environment
- Experimental data indicate that correlation radius of the acoustic field in cross-range direction is of the order of 500 m – 1000 m. Theoretical interpretation based on scattering at internal waves is developed.
- A theory was developed which is applicable to the low-frequency sound propagation in the real ocean up to frequencies of the order of a few hundred Hz
- A theoretical description of the average acoustic field was developed and applied to the estimate of the role of 3-D effects



Statistical Properties of the Acoustic Field in Inhomogeneous Oceanic Environments: *Uncertainties Associated with 3-D and 4-D Effects*



Approach



- **3-D and 4-D effects are often impossible or impractical to model in the deterministic sense**
- **typically weak but not necessarily negligible**
- **described using appropriate perturbation theories within the ray or “vertical modes – horizontal rays” representations of the acoustic field**
- **corrections to acoustic observables due to the 3-D and 4-D effects are expressed in terms of quadratures which involve environmental perturbations and acoustic quantities calculated within 2-D propagation models**
- **propagation of statistical moments of acoustic observables rather than individual realizations of the random acoustic field**

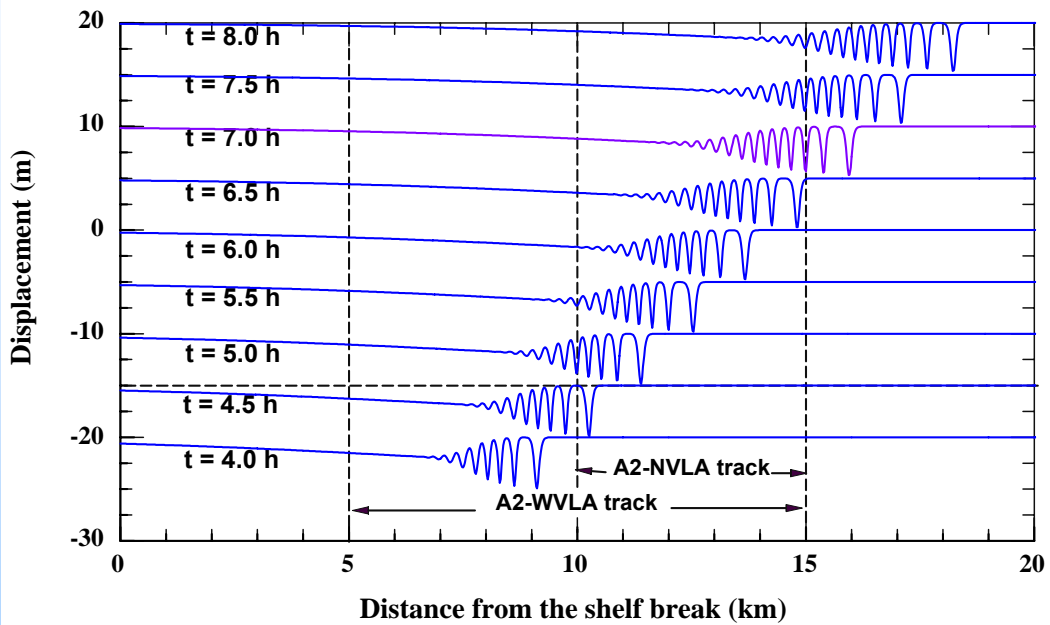


Horizontal refraction due to solitons of internal gravity waves



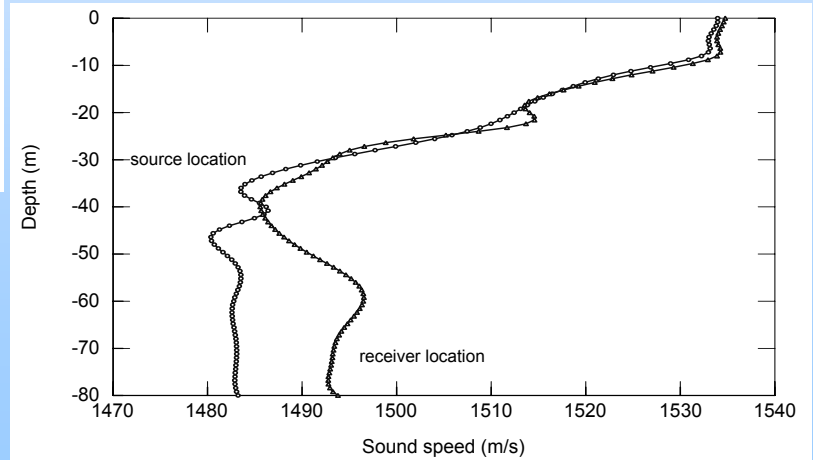
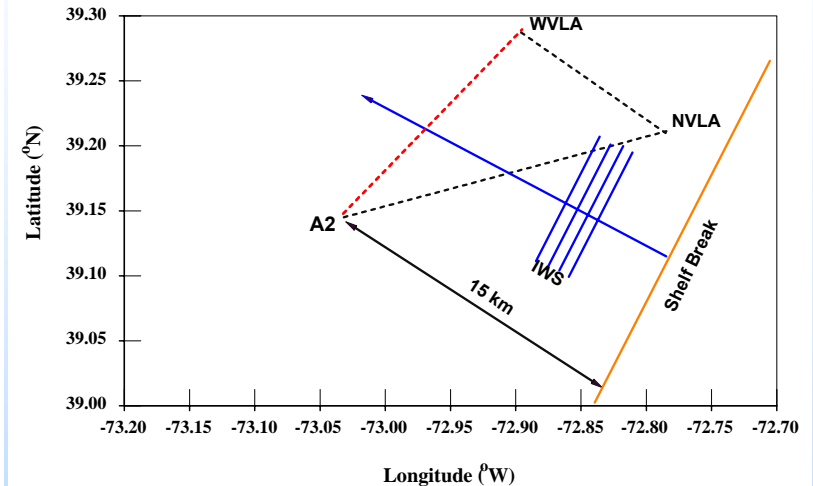
Evolution and propagation of the internal solitary waves at conditions of SWARM experiment

($z = 20 \text{ m}$, $h_1 = 20\text{m}$, $h_2 = 60 \text{ m}$; $\eta_0 = 5 \text{ m}$)



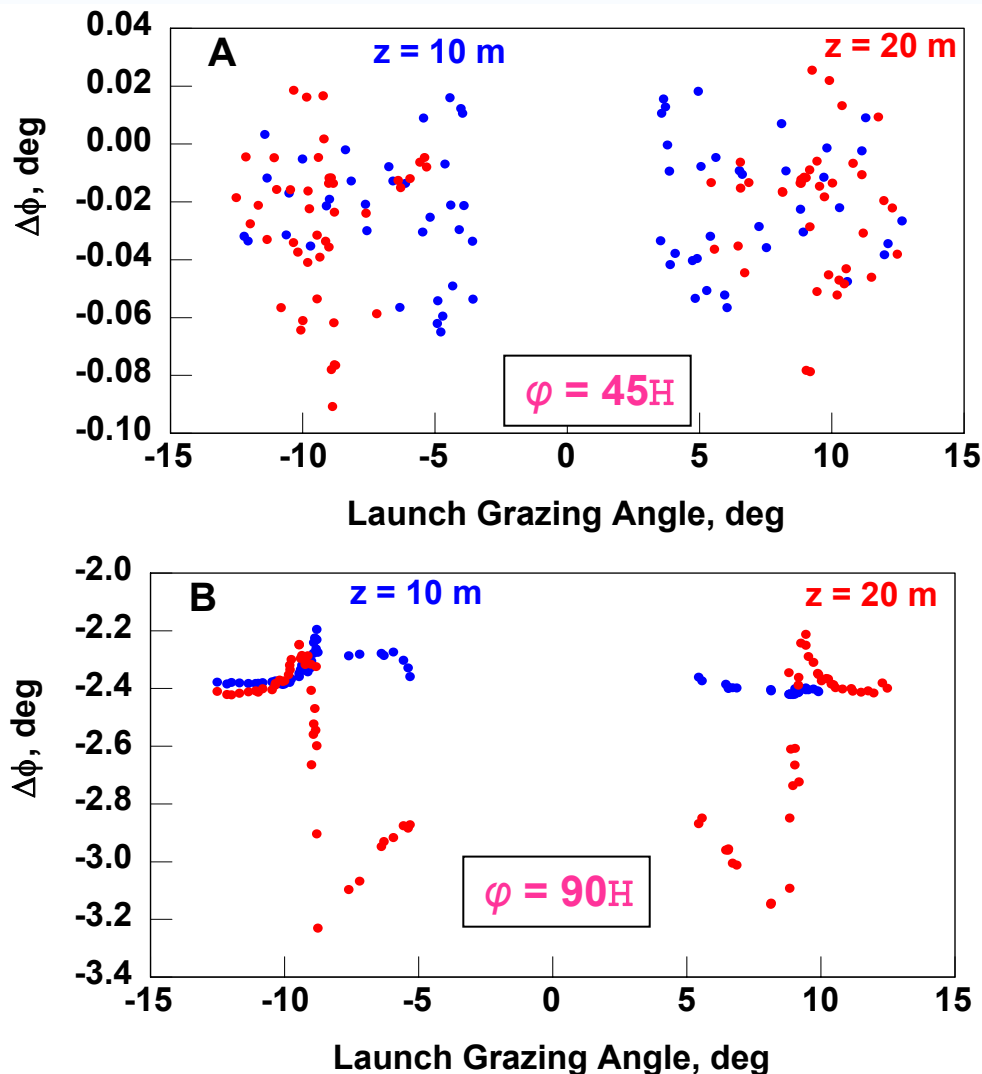
Geometry of the 1995 SWARM Experiment

J. Apel et al., IEEE J. Ocean. Eng., 22(3), pp. 465-499, (1997)
M. Badiey, Y. Mu, J. Lynch, J. Apel, and S. Wolf, IEEE J. Ocean. Eng., 27(1), pp. 117-129 (2002)



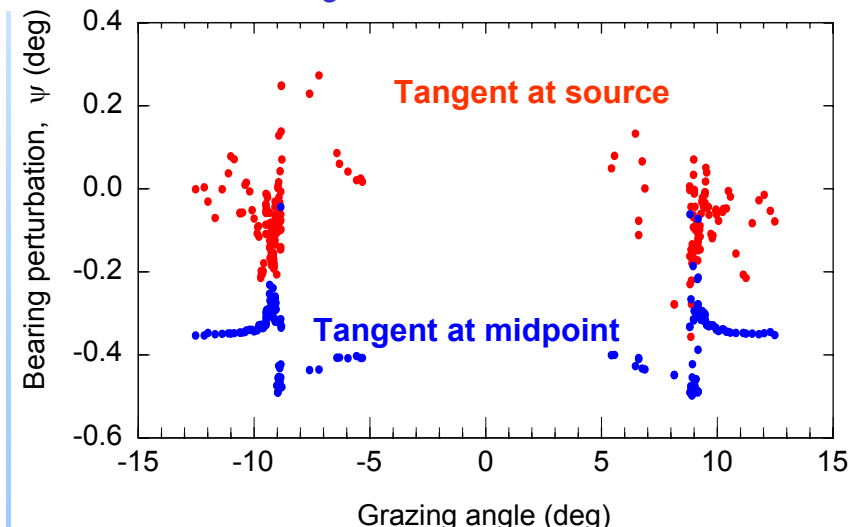


Bearing perturbations due to an IW soliton



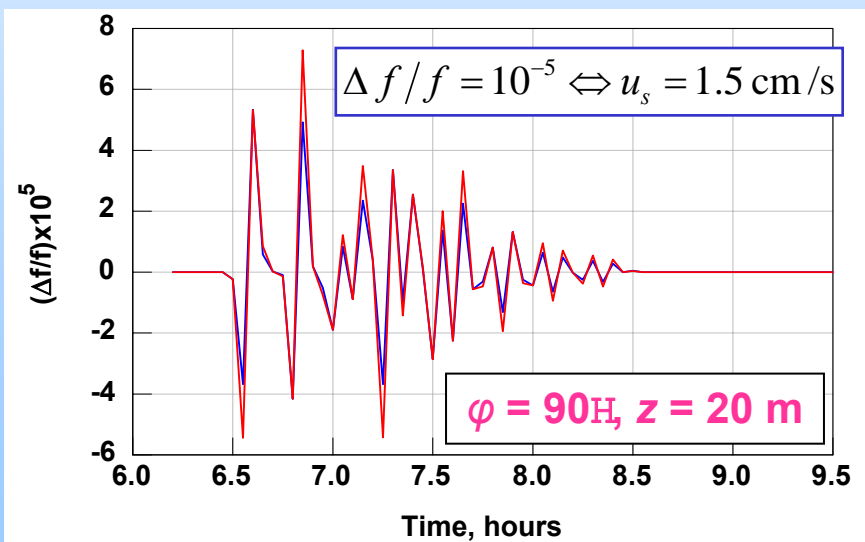
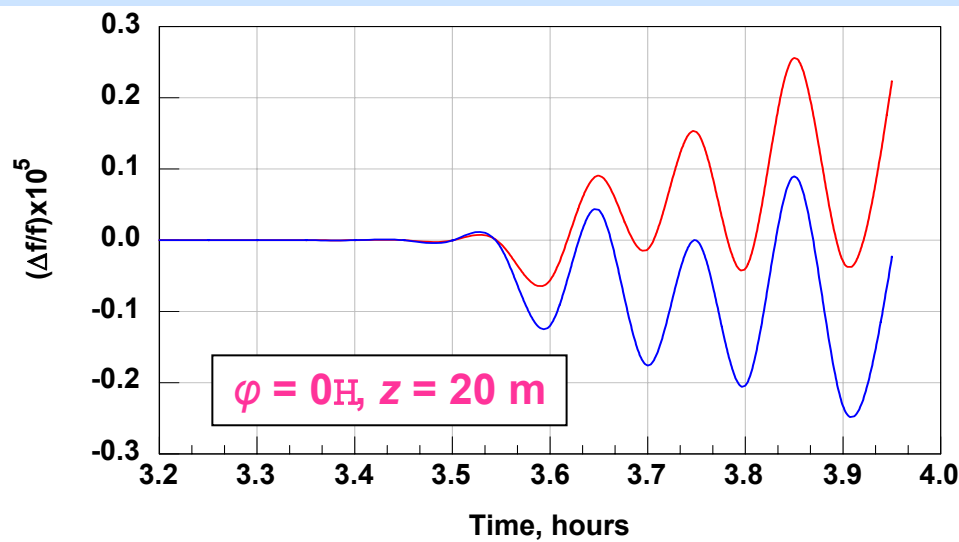
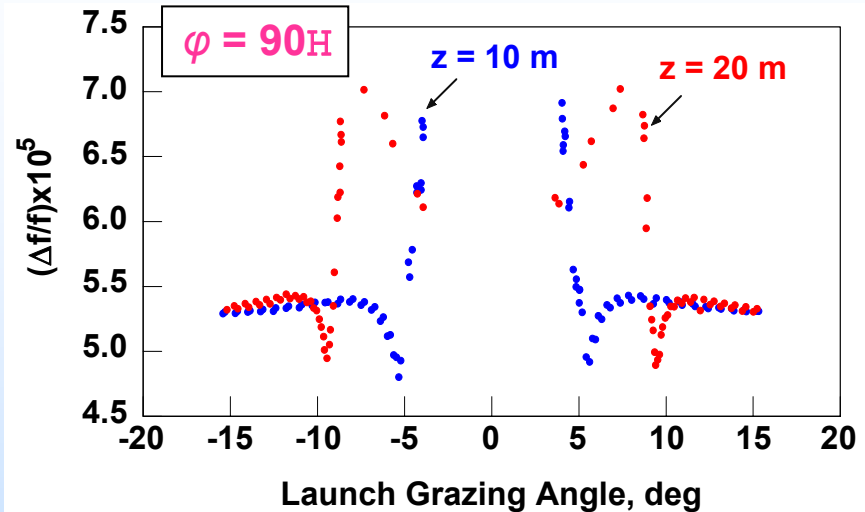
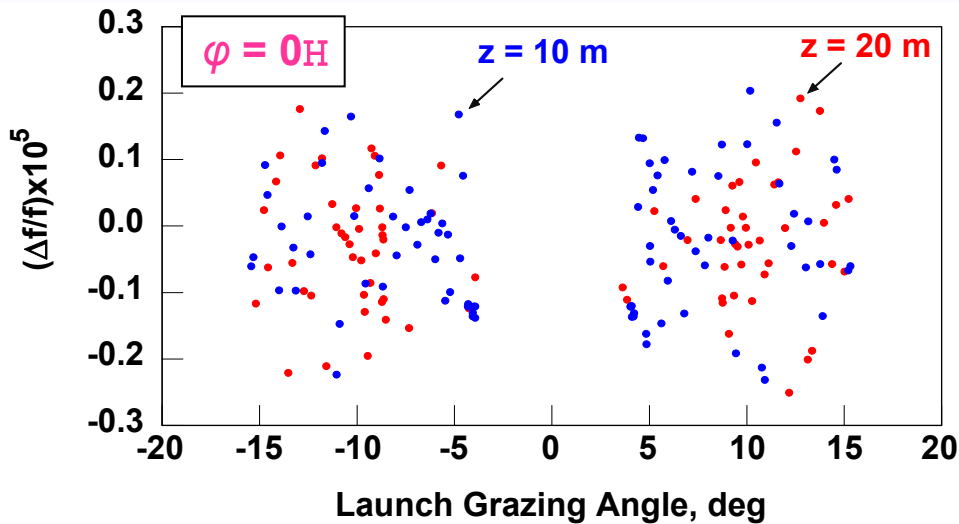
Propagation range $R = 13.5 \text{ km}$,
ocean depth $H = 80 \text{ m}, t = 6.6 \text{ h}$

Cylindrical IW wavefront
with $R_c = 30 \text{ km}; z = 20 \text{ m}$



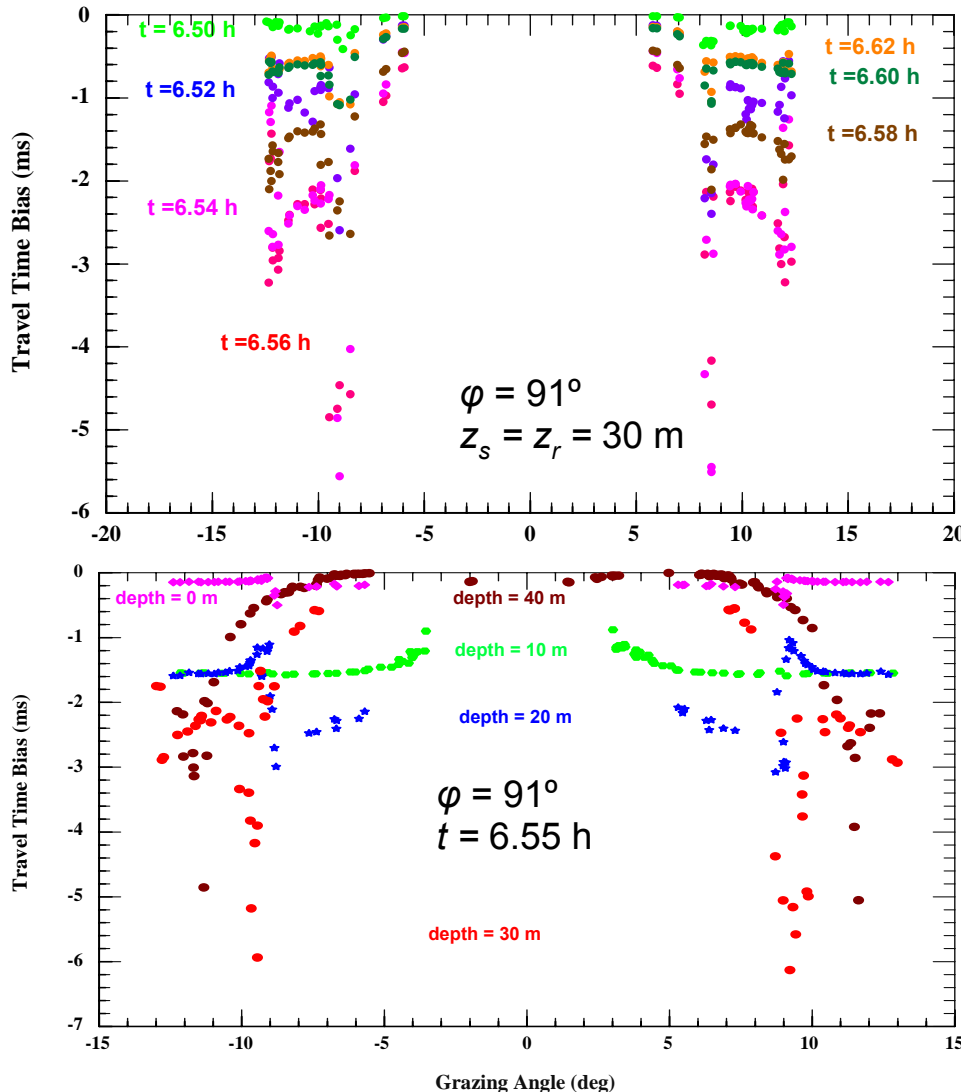


Envelope of frequency fluctuations ($r = 13.5$ km, $z_s = z_r = 20$ m)

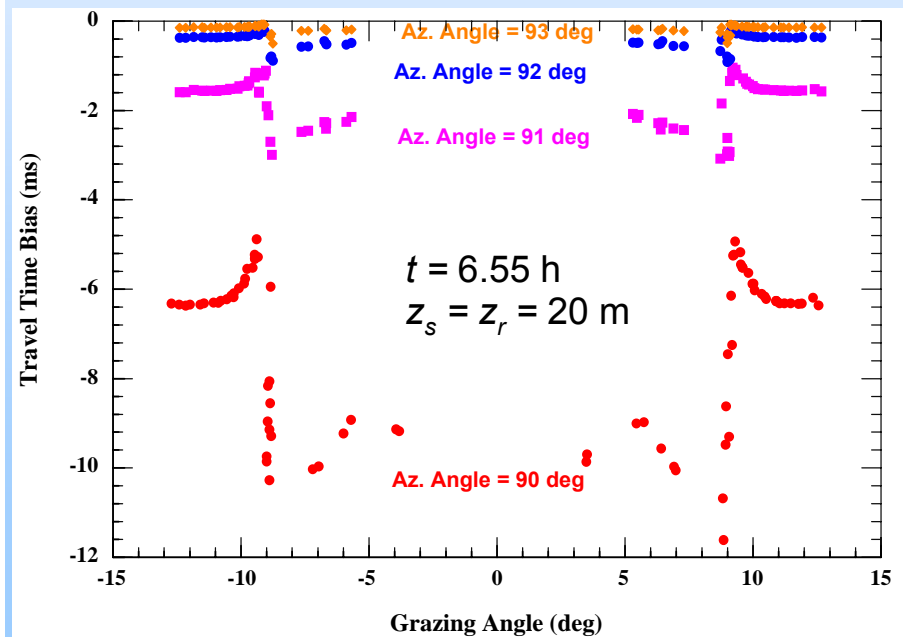


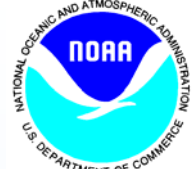


Horizontal refraction due to an IW soliton: ray travel time corrections



Propagation range $R = 13.5 \text{ km}$,
ocean depth $H = 80 \text{ m}$

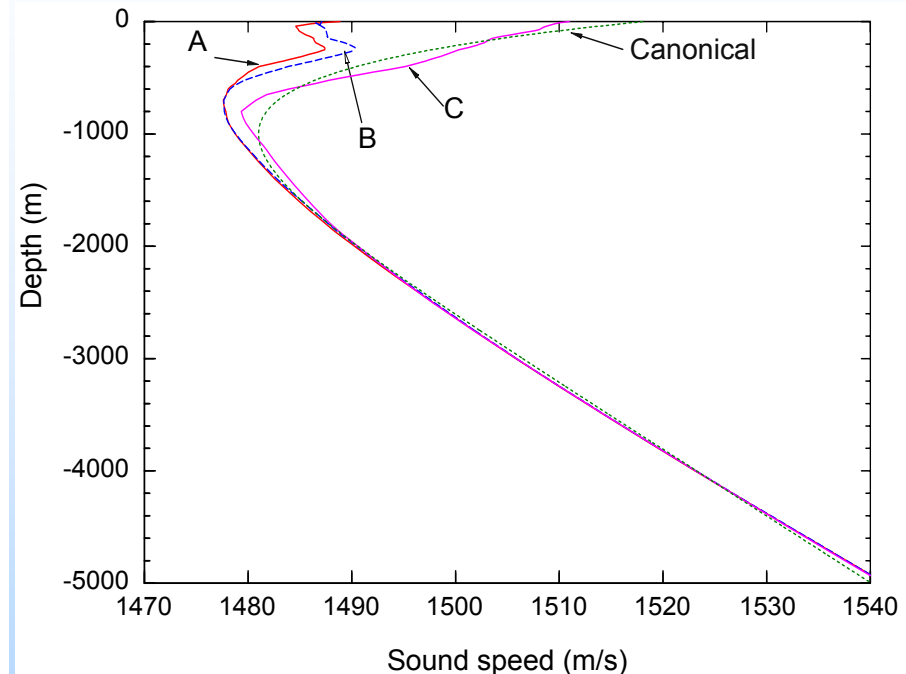
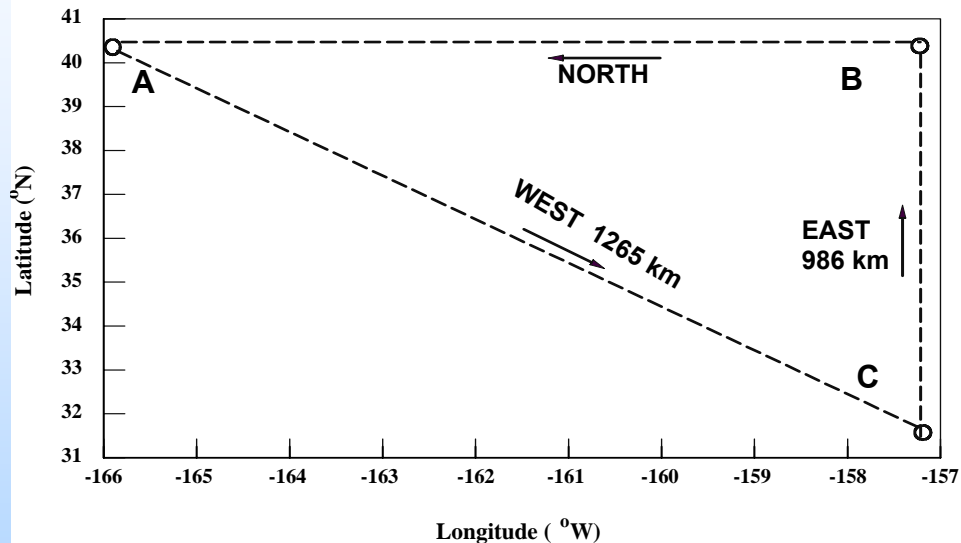




RTE87 experiment



Geometry of the 1987 Reciprocal Transmission Experiment (RTE)
(B. Dushaw, P. Worcester, B. Cornuelle, and B. Howe, JASA, 93(1), pp. 255-275 (1993))



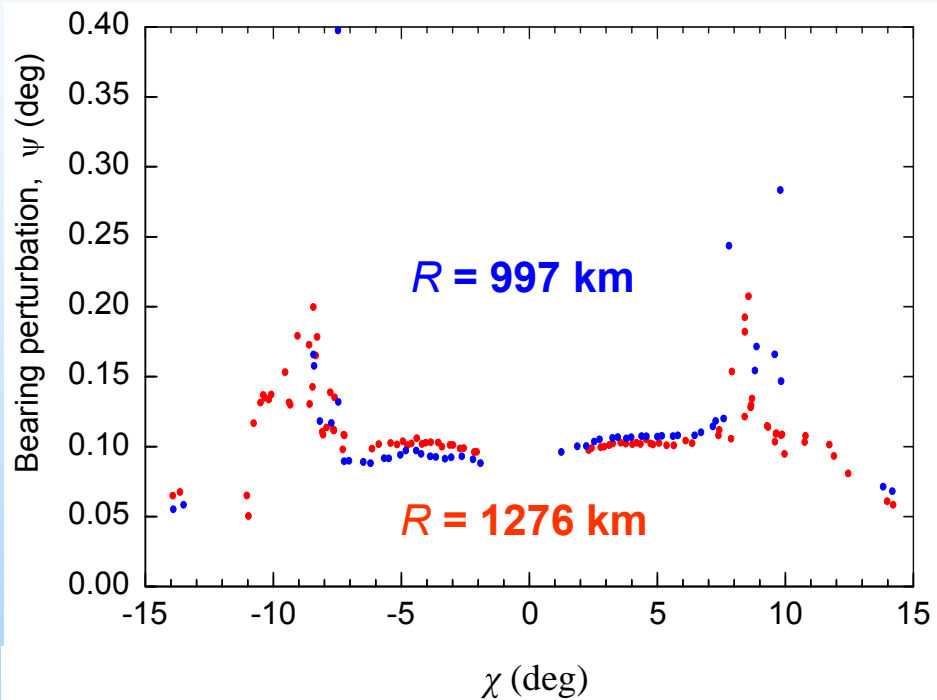
3-D and 4-D acoustic effects in deep water have been modelled assuming RTE87 geometry and three types of hydrological processes: gyre-scale variations in the sound speed, mesoscale inhomogeneities, and internal gravity waves with the GM spectrum.



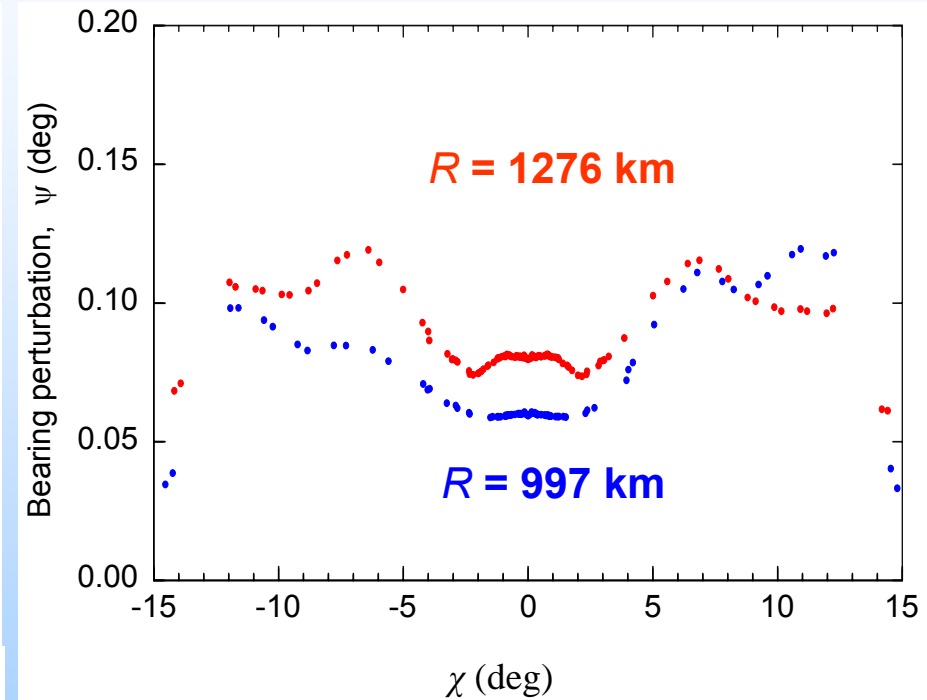
Mesoscale-induced bearing perturbations



RTE87



Canonical sound speed profile



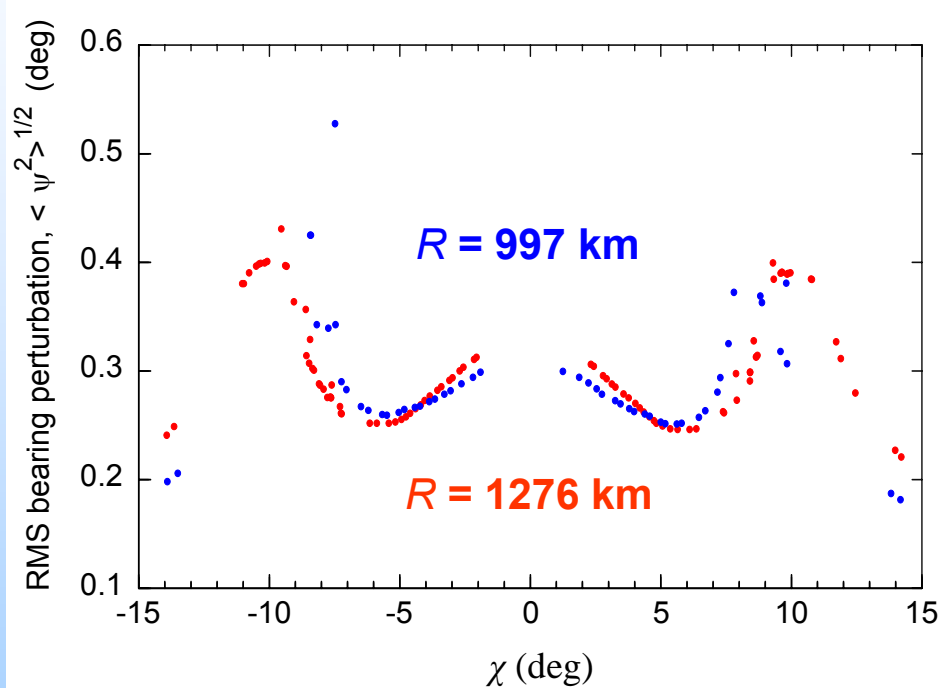
Source and receiver depth: $z_s = z_r = 1 \text{ km}$



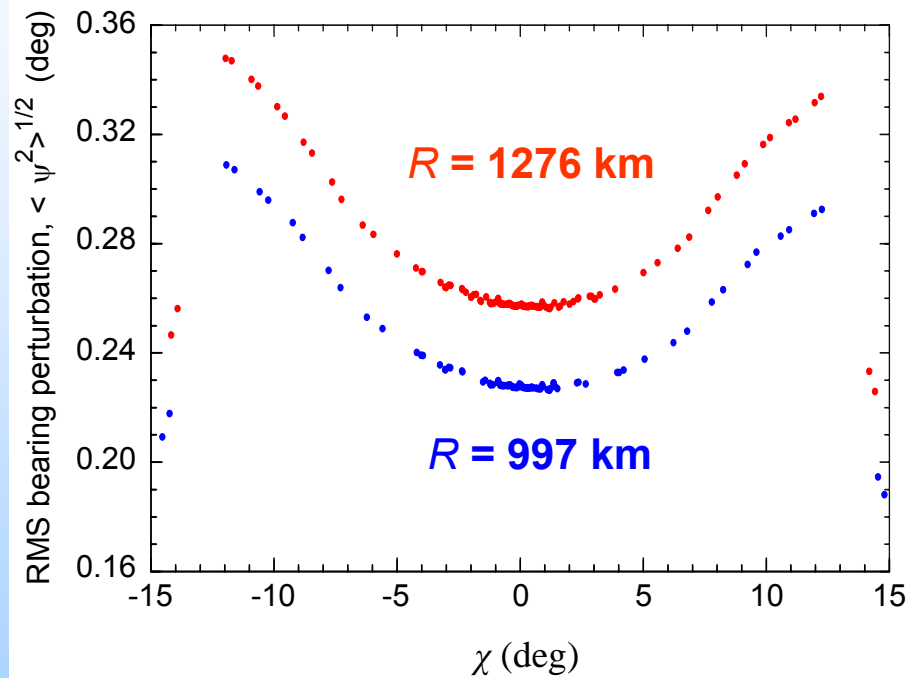
IW-induced fluctuations of the horizontal refraction angle



RTE87



Canonical sound speed profile



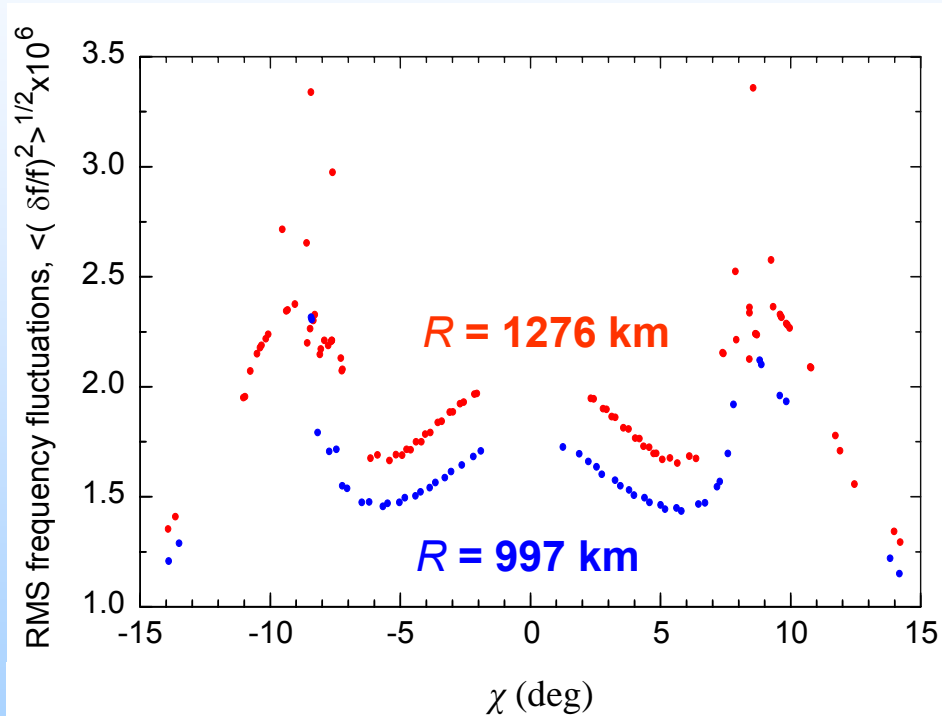
Source and receiver depth: $z_s = z_r = 1$ km



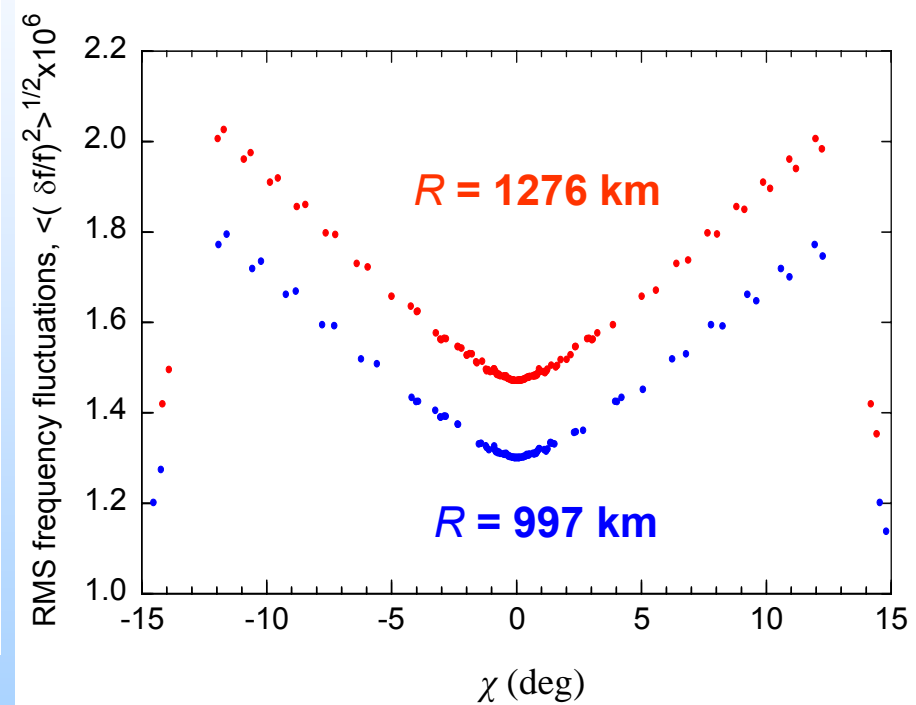
Acoustic frequency wander in deep ocean



RTE87



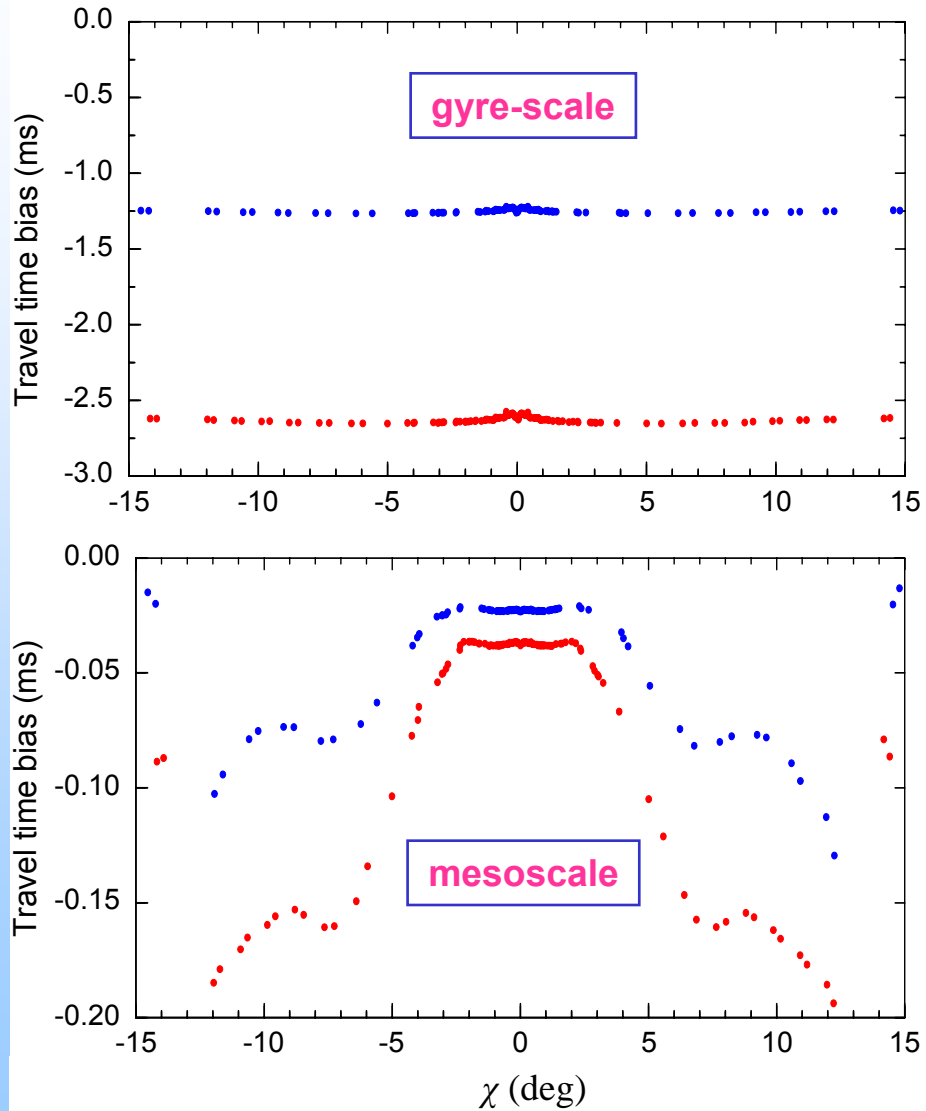
Canonical sound speed profile



Source and receiver depth: $z_s = z_r = 1 \text{ km}$

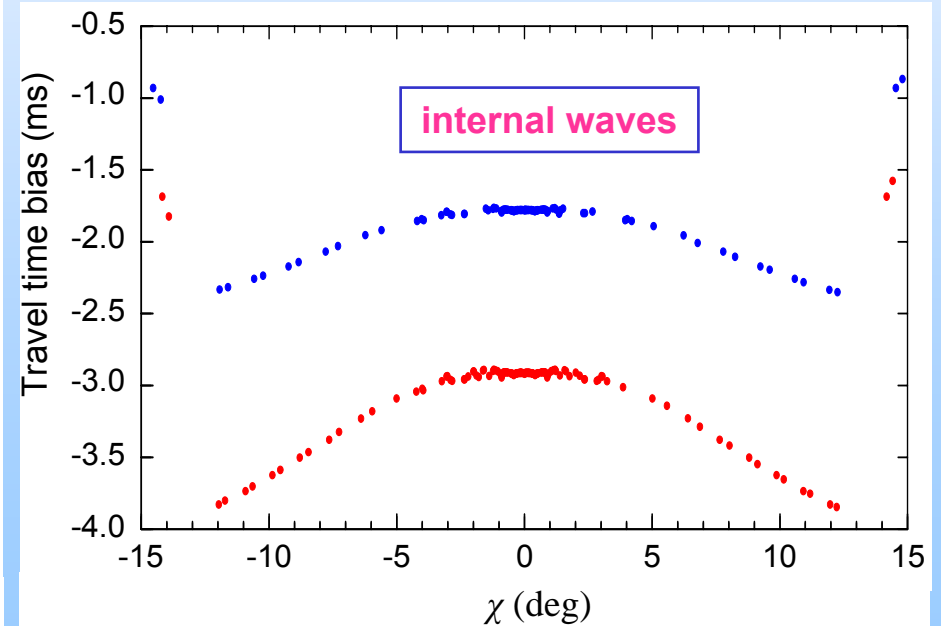


Acoustic travel-time correction due to horizontal refraction (1)



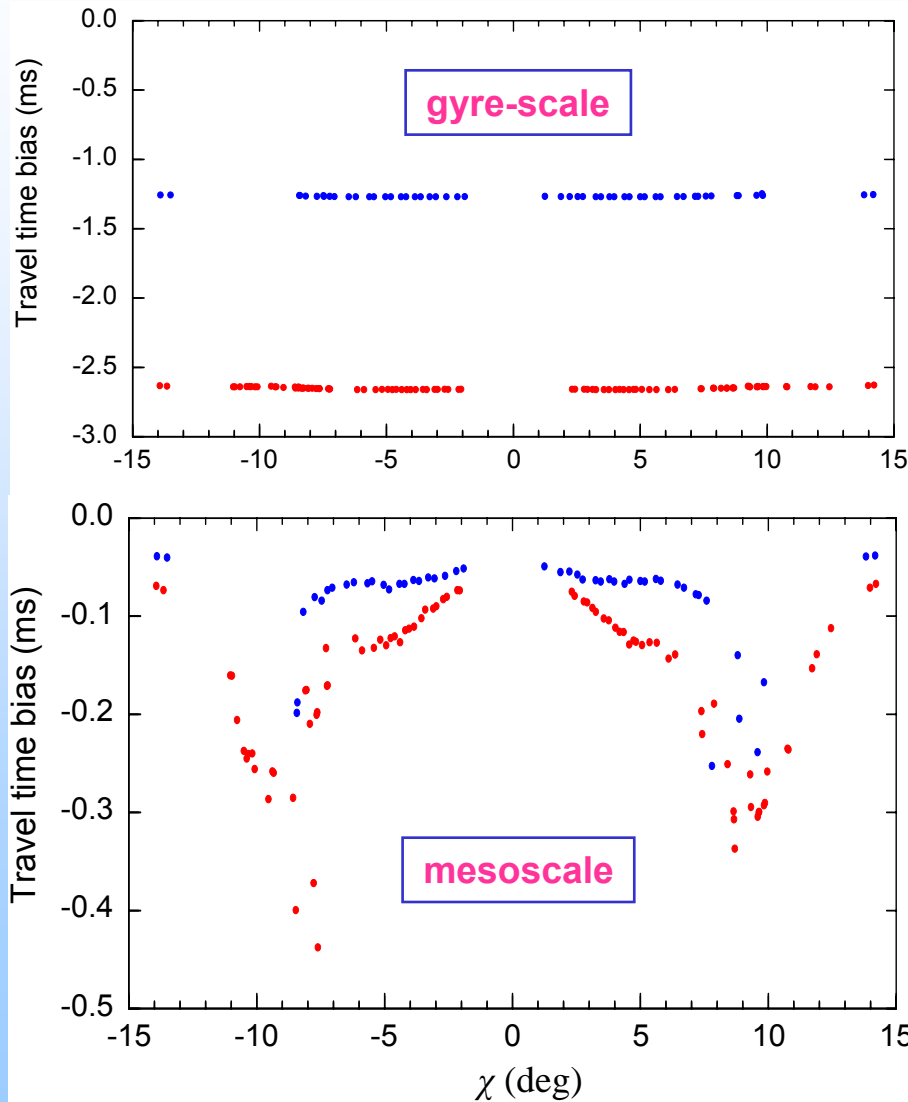
Canonical sound speed profile

Source and receiver
depth: $z_s = z_r = 1$ km.
 $R = 1276$ km and 997 km



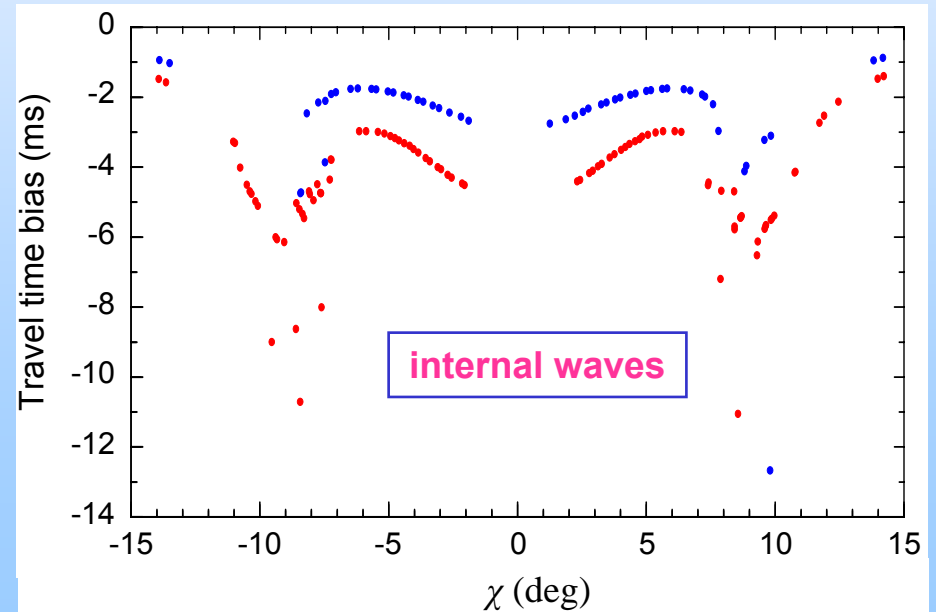


Acoustic travel-time correction due to horizontal refraction (2)



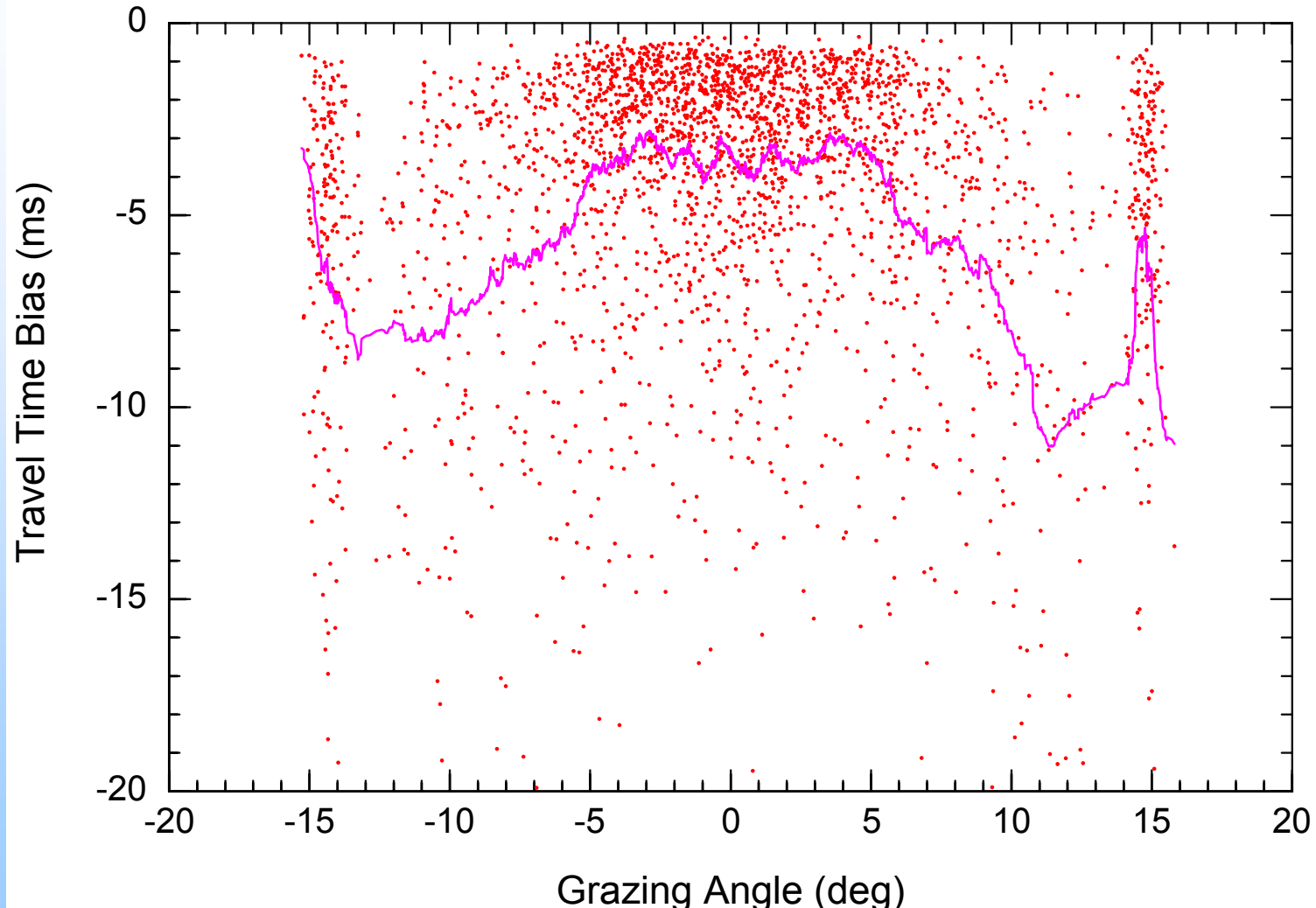
RTE87 background sound speed

Source and receiver depth: $z_s = z_r = 1$ km.
 $R = 1276$ km and 997 km



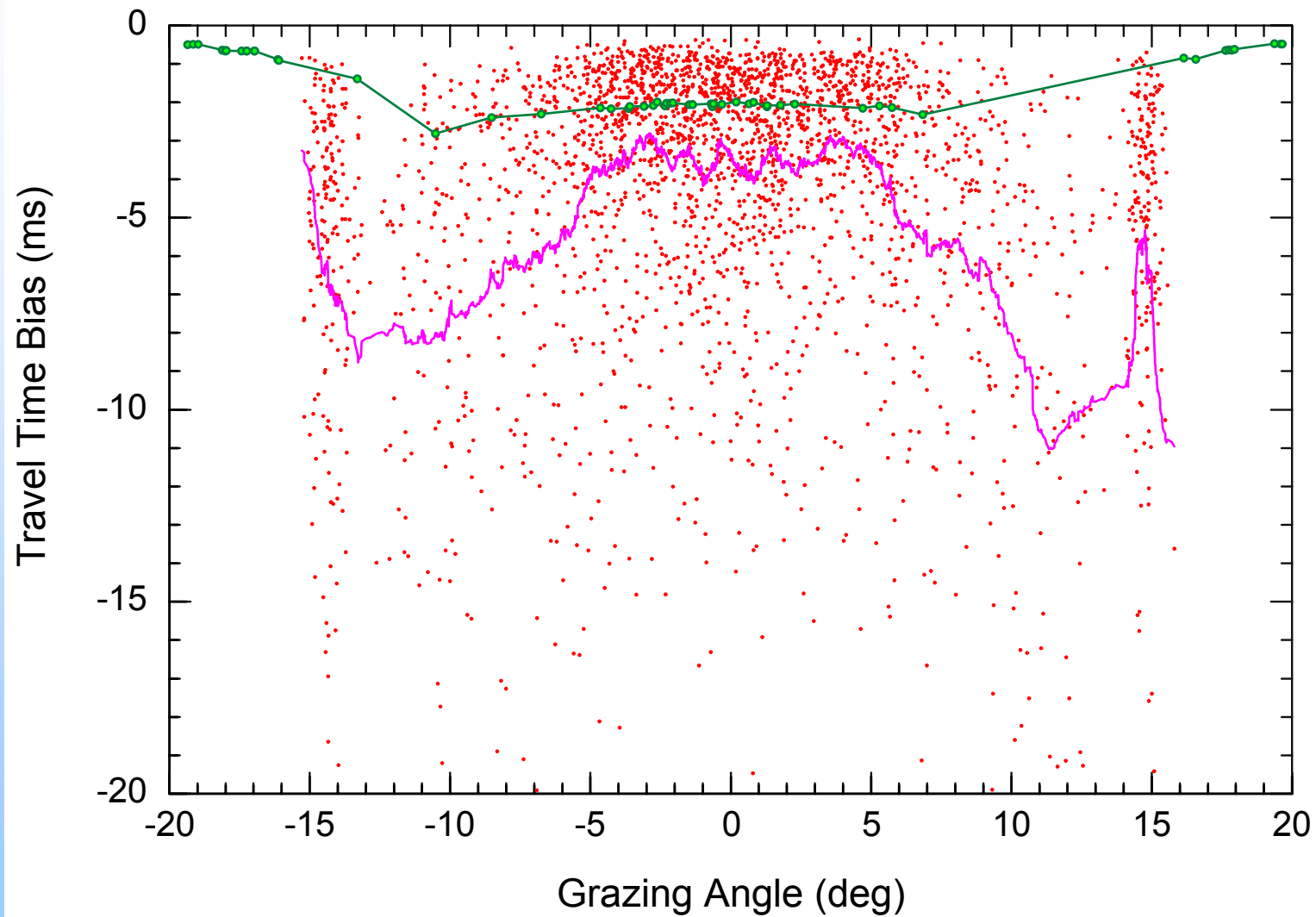


Monte Carlo simulations of the horizontal refraction induced by internal waves



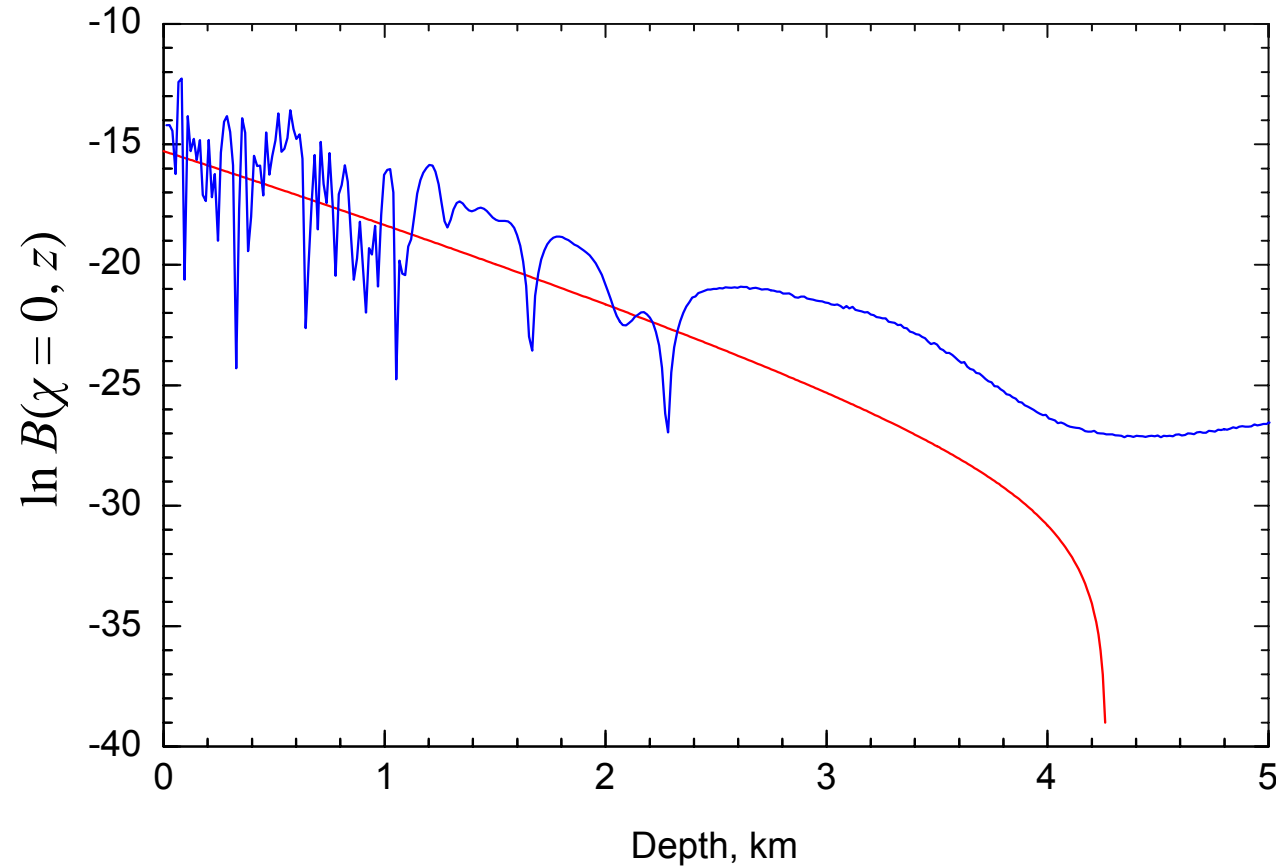


Monte Carlo vs. direct calculation of the travel time bias (1)





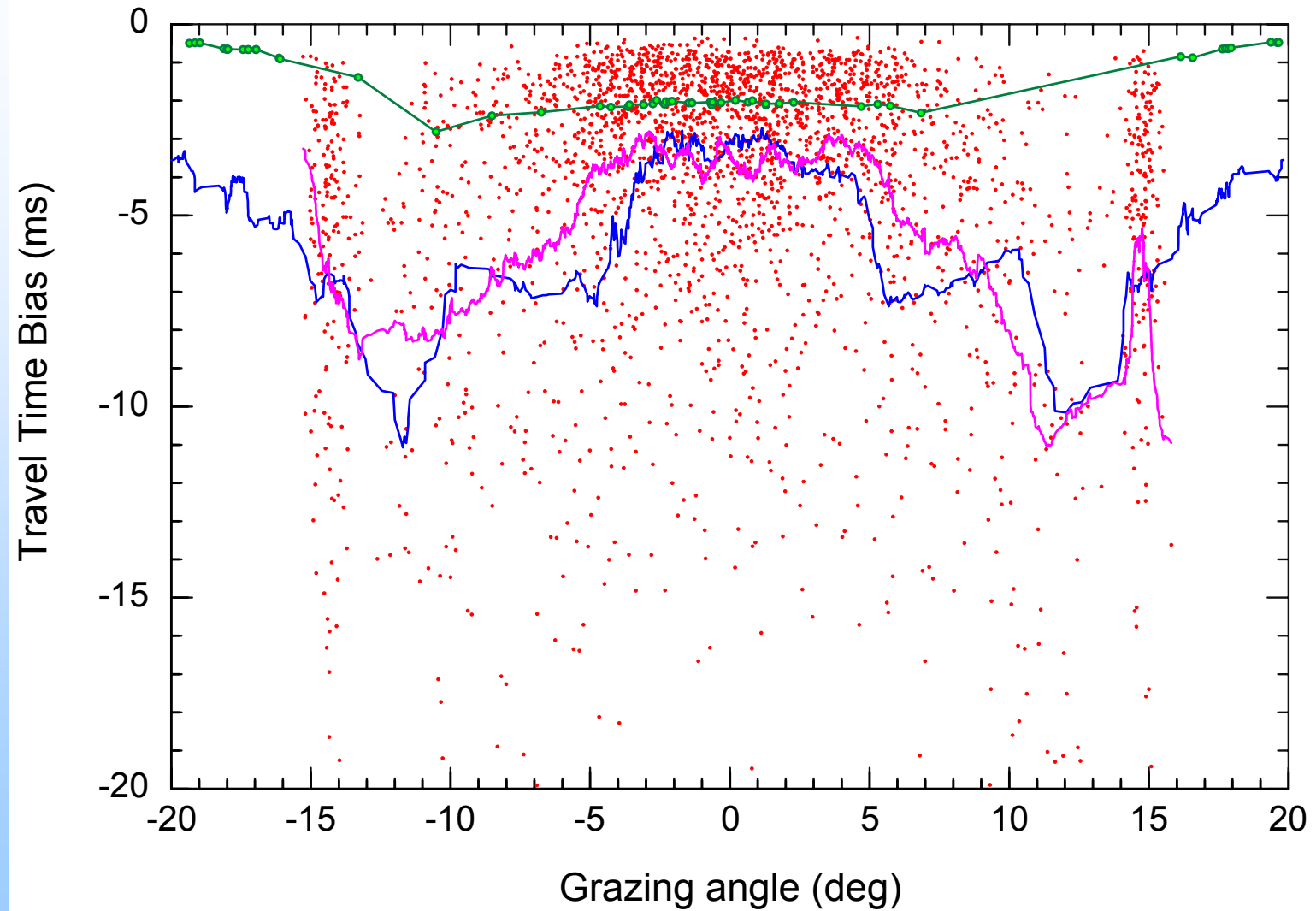
Two models of sound speed fluctuations



$$B(\chi, z) = \frac{1}{2} \int_{-\infty}^{+\infty} W(a \cos \chi, 0, a \sin \chi; z) da$$



Monte Carlo vs. direct calculation of the travel time bias (2)

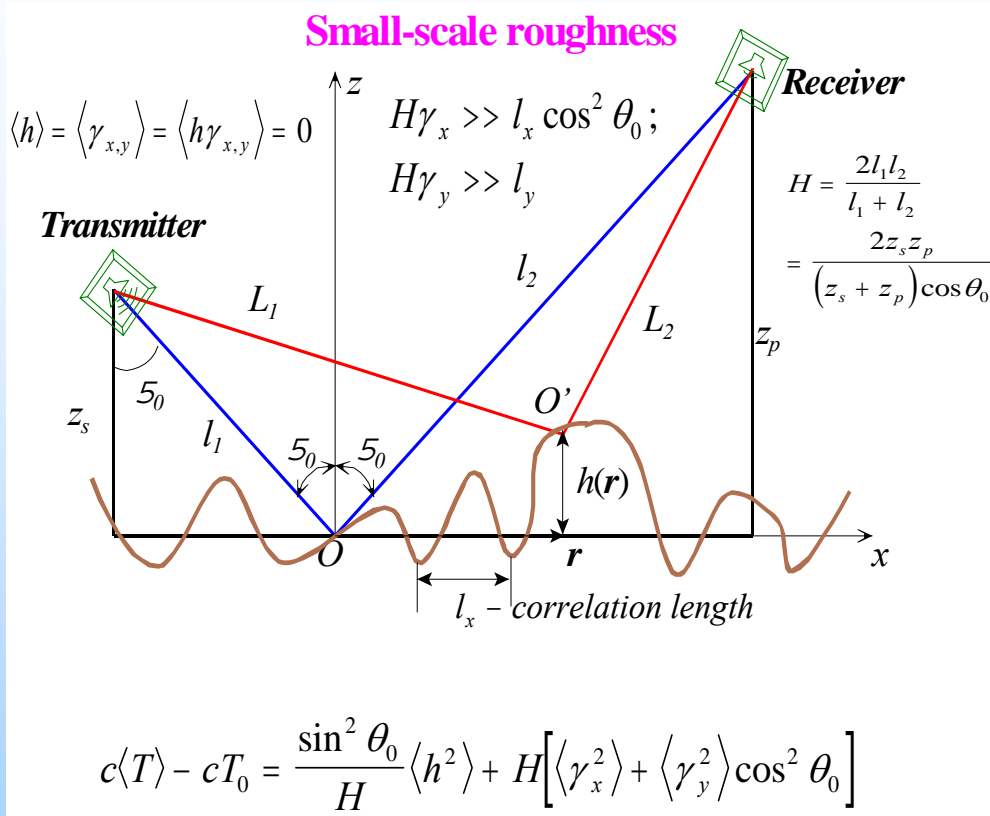




Statistical Properties of the Acoustic Field in Inhomogeneous Oceanic Environments: *Uncertainties in the Acoustic Field Associated with Rough Surface Scattering*



Travel-Time Statistics for Waves Scattered at a Rough Surface



PDF of random travel times

$$\tau = (T - T_0)/T_0, \quad b = \langle \gamma_y^2 \rangle \cos^2 \theta_0 / \langle \gamma_x^2 \rangle$$

Large-scale roughness:

$$W(\tau) = \frac{1}{\sqrt{2\pi\langle \tau^2 \rangle}} \exp\left(-\frac{(\tau - \langle \tau \rangle)^2}{2\langle \tau^2 \rangle}\right)$$

$$\langle \tau^2 \rangle = 4 \cos^2 \theta \langle h^2 \rangle / (l_s + l_p)^2$$

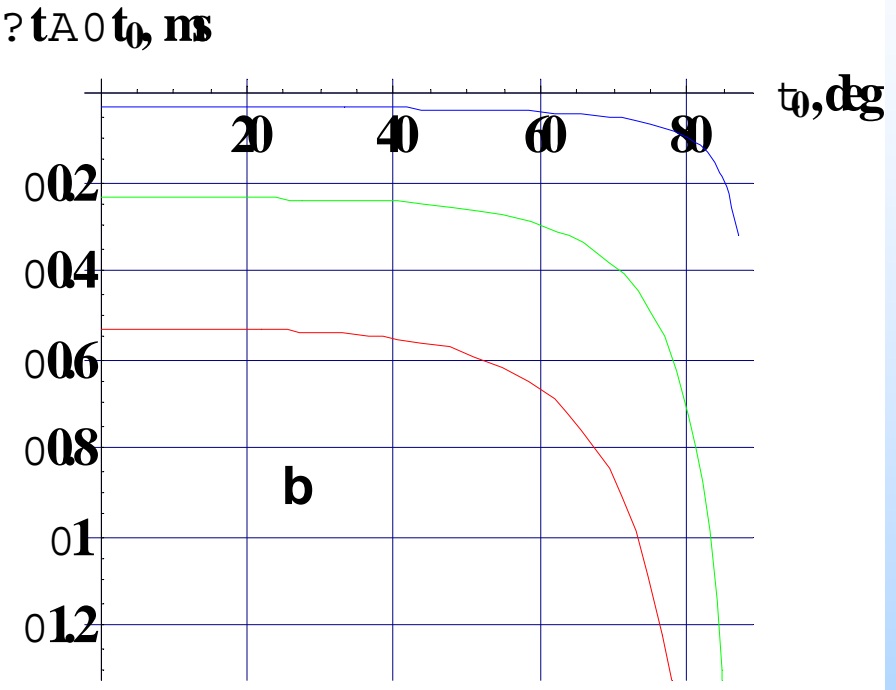
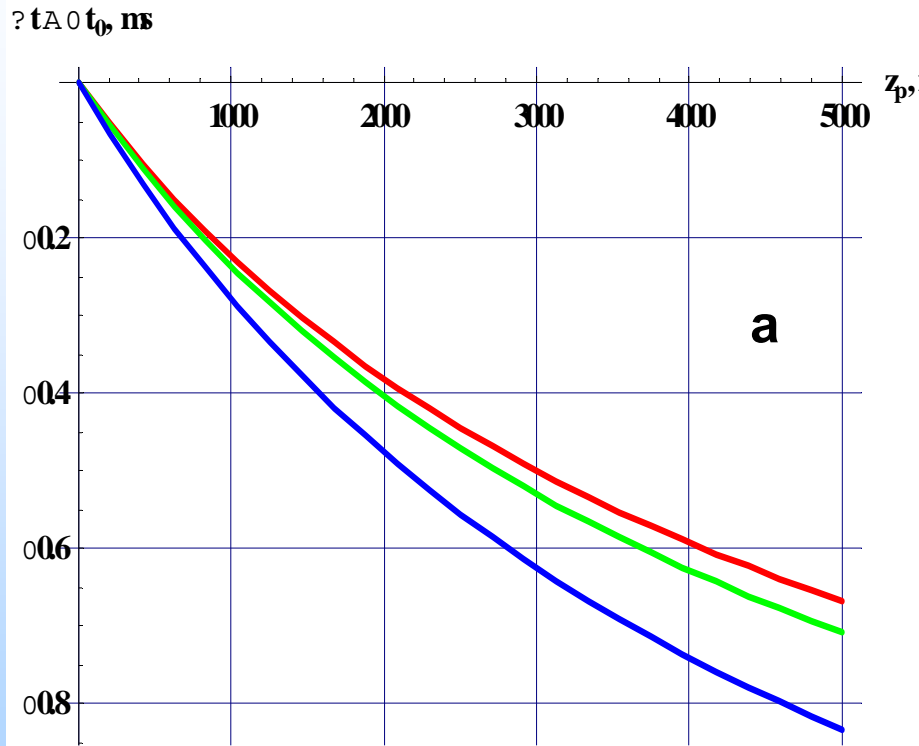
$$\langle \tau \rangle = \frac{2\langle h^2 \rangle \sin^2 \theta}{(l_s + l_p)^2} \mp \frac{2l_s l_p}{(l_s + l_p)^2} (\langle \gamma_x^2 \rangle + \langle \gamma_y^2 \rangle \cos^2 \theta)$$

Small-scale roughness:

$$W(a) = \frac{1}{\sqrt{b}} \exp\left(-a \frac{1+b}{2b}\right) I_0\left(a \frac{1-b}{2b}\right), \quad a = \frac{\tau(l_s + l_p)^2}{4l_s l_p \langle \gamma_x^2 \rangle}$$



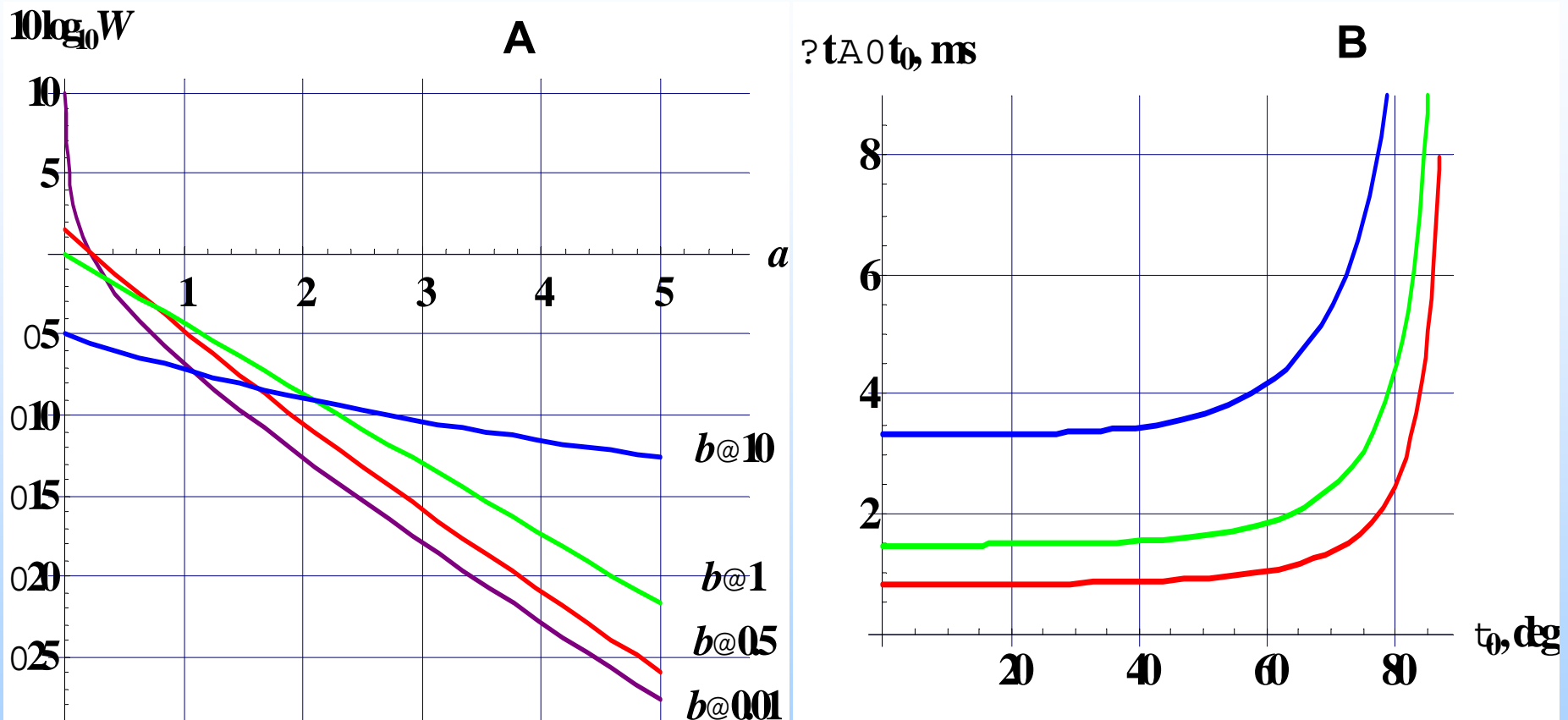
Travel-Time Statistics for Waves Scattered at a Large-Scale Rough Surface



Travel-time bias of reflected acoustic waves as a function of (a) the receiver depth ($t_0 = 0^\circ$, 45° , and 60° , $L = 200$ m, $z_s = 5000$ m, $\langle h^2 \rangle = 4$ m 2) and (b) the angle of incidence ($L = 100$ m, 150 m, and 400 m, $z_p = z_s = 1000$ m)



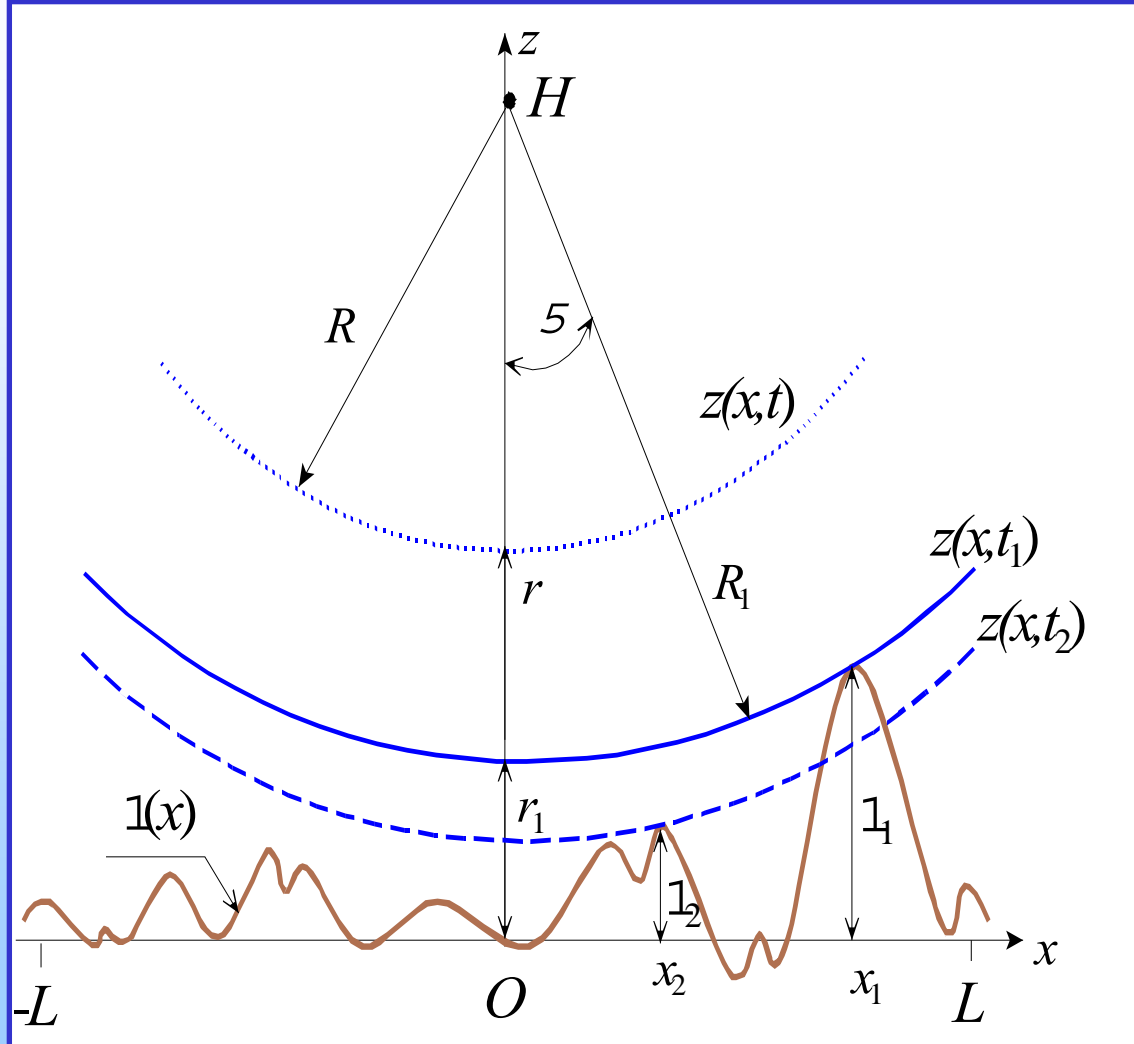
Travel-Time Statistics for Waves Scattered at a Small-Scale Rough Surface



Travel-time PDF (A) and bias of reflected acoustic wave as a function of the angle of incidence (B) ($L = 20$ m, 15 m, and 10 m, $z_p = z_s = 1000$ m, $\langle h^2 \rangle = 0.25$ m²)



First arrivals of acoustic pulses backscattered from rough surfaces



Travel time of
the first arrival:

$$t_1 = 2R_1/c$$

Time scale:

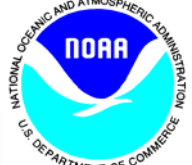
$$2\sigma/c$$

Dimensionless travel
time difference:

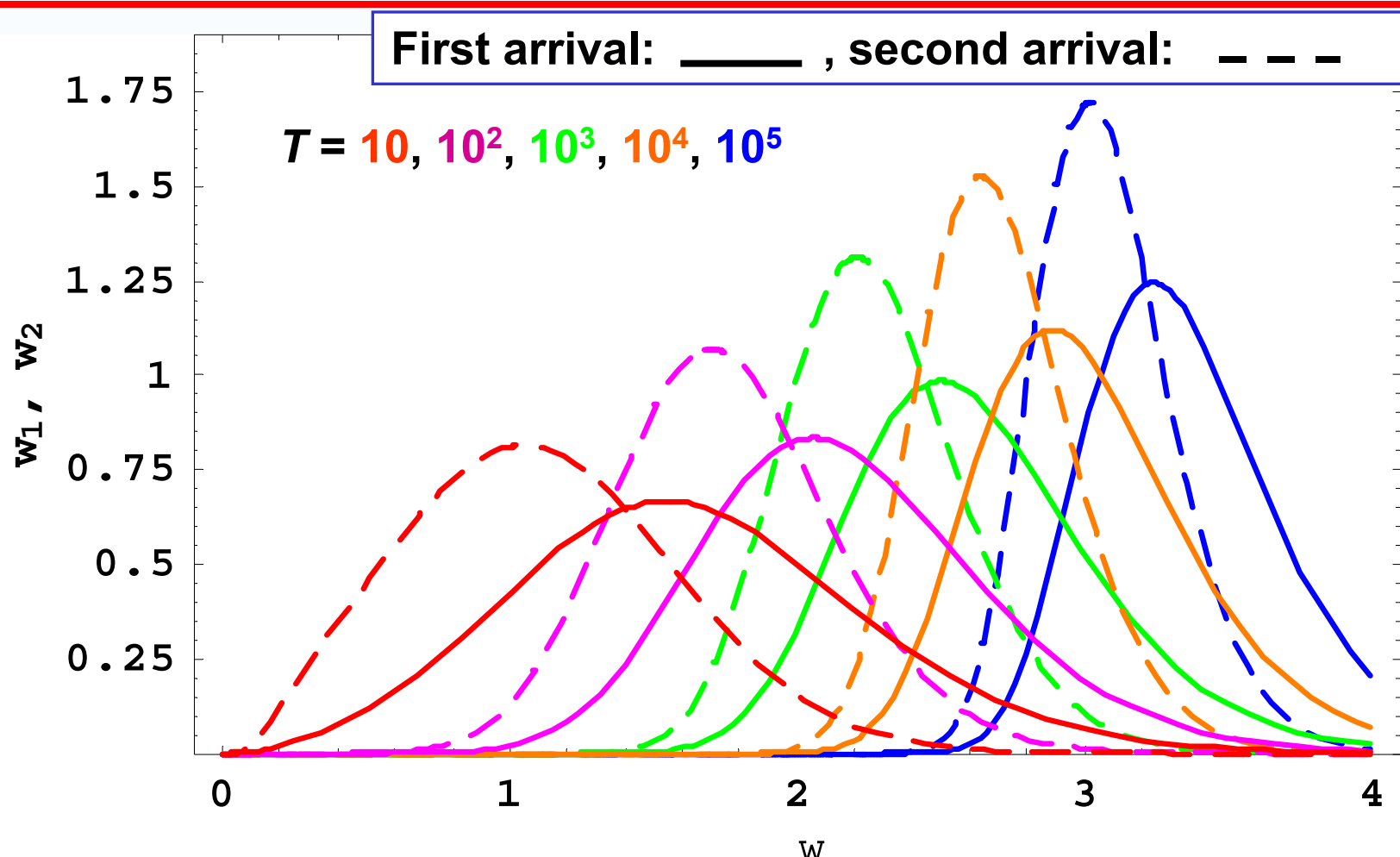
$$\tau_1 = \left(\frac{2\sigma}{c}\right)^{-1} \left(\frac{2H}{c} - t_1 \right) = \frac{r_1}{\sigma}$$

Key dimensionless
parameter:

$$T = \gamma_0^2 H / 2\pi\sigma$$



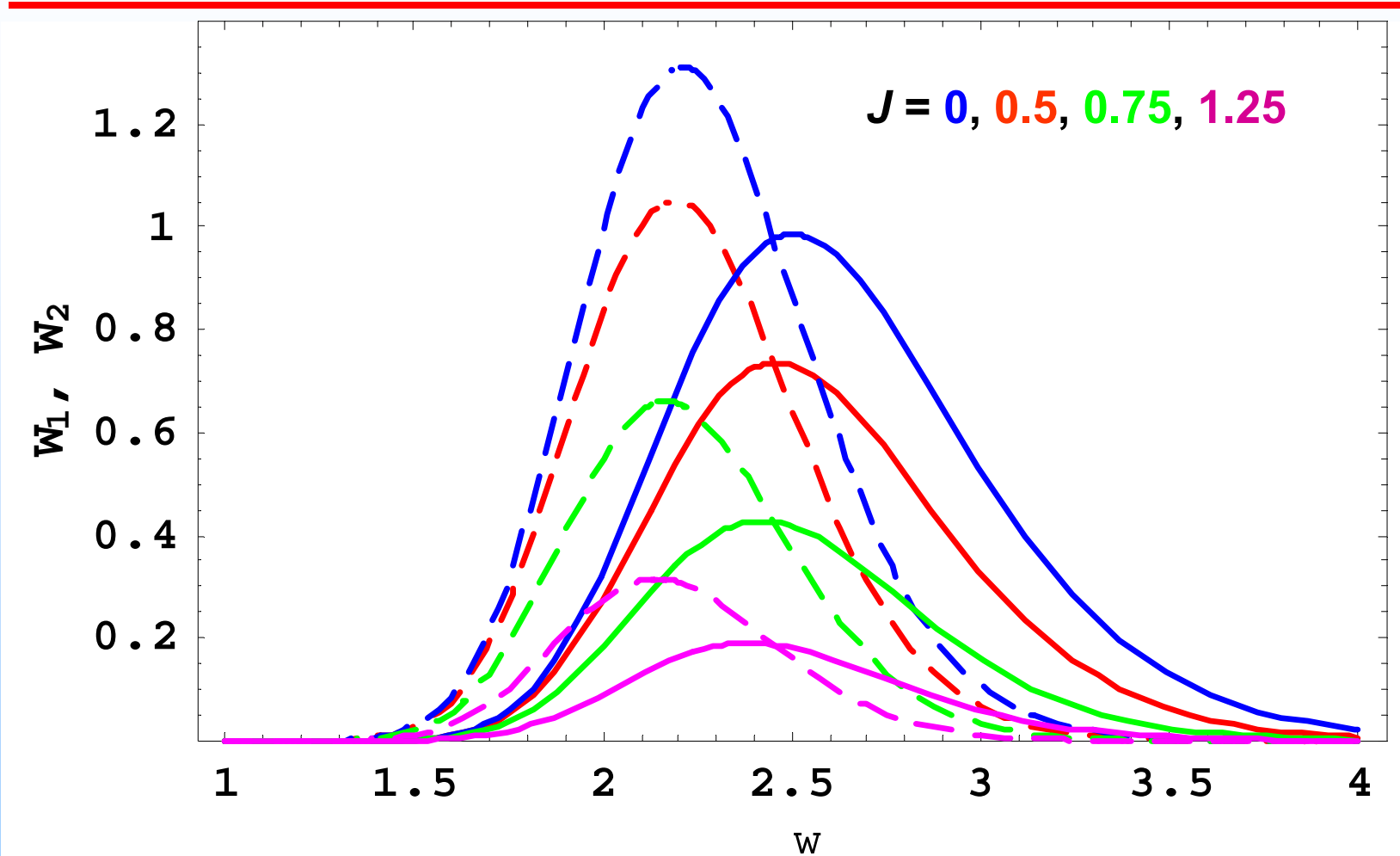
The travel time PDFs of early arrivals



$$\tau_{1m} \approx \sqrt{\ln T + 0.733}, \quad \tau_{2m} \approx \sqrt{\ln T - 1.038}, \quad \tau_{1m} - \tau_{2m} \approx 0.885/\sqrt{\ln T}$$



Travel times of arrivals exceeding an intensity threshold





PUBLICATIONS (1)



Papers in peer-reviewed journals

1. O. A. Godin, A 2-D description of sound propagation in a horizontally-inhomogeneous ocean, *J. Comput. Acoustics* **10**, 123-151 (2002)
2. O. A. Godin, Coupled-mode sound propagation in a range-dependent, moving fluid, *J. Acoust. Soc. Am.* **111**, 1984-1995 (2002)
3. O. A. Godin, On effective quiescent medium for sound propagating through an inhomogeneous, moving fluid, *J. Acoust. Soc. Am.* **112**, 1269-1275 (2002)
4. O. A. Godin, Wide-angle parabolic equations for sound in a 3-D inhomogeneous, moving medium, *Doklady Physics* **47**, p. 643-647 (2002)
5. O. A. Godin, On sound propagation in a nonstationary ocean, *Doklady Physics* **47**, p. 639-642 (2002)
6. O. A. Godin, Approximate description of sound fields in a time-dependent ocean, *Izv. Atmos. Ocean. Phys.* **38**, p. 700-705 (2002)
7. O. A. Godin, Systematic distortions of signal propagation times in random inhomogeneous media, *Doklady Physics* **48**, p. 389-394 (2003)
8. O. A. Godin and I. M. Fuks, Travel-time statistics for signals scattered at a rough surface, *Waves in Random Media* **13**, p. 205-221 (2003)

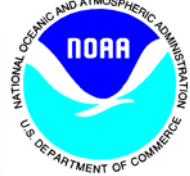


PUBLICATIONS (2)



Papers in peer-reviewed journals (continued)

9. A. Voronovich, Strong solitary internal waves in a 2.5-layer model, *J. Fluid Mech.* **474**, p. 85-94 (2002). DOI: 10.1017/S0022112002002744
10. A. G. Voronovich and O. A. Godin, Fermat principle for a non-stationary medium, *Phys. Rev. Lett.*, **91** (4), p. 044302_1-044302_4. (2003). DOI: 10.1103/PhysRevLett.91.044302
11. O. A. Godin, On derivation of differential equations of coupled-mode propagation from the reciprocity principle, *J. Acoust. Soc. Am.* **114** (6), p. 3016-3019 (2003)
12. O. A. Godin and A. G. Voronovich, Fermat's principle for non-dispersive waves in nonstationary media, *Proc. R. Soc. Lond. A* **460** (2046), p. 1631-1647 (2004). DOI: 10.1098/rspa.2003.1231
13. I. M. Fuks and O. A. Godin, Probability distribution of the travel time and intensity of the two first arrivals of a short pulse backscattered by a rough surface, *Waves in Random Media* (2004) [in press]
14. O. A. Godin, V. U. Zavorotny, A. G. Voronovich, and V. V. Goncharov, Refraction of sound in a horizontally-inhomogeneous, time-dependent ocean, submitted to *IEEE J. Oceanic Engineering* (2004)
15. O. A. Godin, V. U. Zavorotny, A. G. Voronovich, and V. V. Goncharov, Random horizontal refraction of sound induced by internal gravity waves, to be submitted to *J. Acoust. Soc. Am.* (2004) [in preparation]



PUBLICATIONS (3)



Conference papers

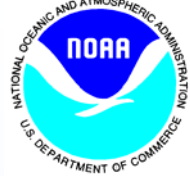
1. O. A. Godin, Modeling of sound propagation in a time-dependent ocean. In: *Ocean Acoustics. Proceedings of the 9th L. M. Brekhovskikh's Conference* (GEOS, Moscow, 2002), p. 112-115 (in Russian).
2. O. A. Godin, Acoustic fields in ocean with currents: Effective sound speed approximation, its justification and extension. In: *Proceedings of the Sixth European Conference on Underwater Acoustics (24-27 June 2002, Gdansk, Poland)* (Gdansk University of Technology, Gdansk, 2002), p. 387-390.
3. O. A. Godin, Random horizontal refraction and biases in ray travel time and mode phase. In: *Proceedings of the Sixth European Conference on Underwater Acoustics (24-27 June 2002, Gdansk, Poland)* (Gdansk University of Technology, Gdansk, 2002), p. 315-318.
4. O. A. Godin, Modeling the effects of horizontal refraction and medium non-stationarity in ocean acoustics. In: *Theoretical and Computational Acoustics 2001* ed. by E-C.Shang, Q. Li, and T. F. Gao (World Scientific, Singapore, 2002), p. 35-49
5. I. M. Fuks and O. A. Godin, Statistical parameters of the travel time for signals reflected or refracted at a rough surface. In: *Proceedings of the International Geoscience and Remote Sensing Symposium - IGARSS 2003 (21-25 July 2003, Toulouse, France)*, vol. 7, p. 4207-4210
6. O. A. Godin, A. G. Voronovich, and V. U. Zavorotny, Coherent scattering of underwater sound and its implications for ocean remote sensing. In: *Proceedings of the Tenth International Congress on Sound and Vibration (7-10 July 2003, Stockholm, Sweden)*, vol. 5, p. 2539-2546
7. I. M. Fuks and O. A. Godin, Travel time and intensity statistics of the pulsed signals backscattered by a rough surface. In: *Proceedings of the 2004 IEEE Antennas and Propagation Society Conference (20-26 June 2004, Monterey, CA)* [in press]



Accomplishments



- uncertainties in acoustic observables associated with cross-range environmental gradients and internal-wave induced sound-speed time-dependence have been quantified;
- numerical algorithm has been developed to predict statistical moments of acoustic signals in horizontally-inhomogeneous waveguides with time-dependent parameters;
- hydrodynamic theory has been developed for a dynamic description of strongly non-linear internal wave solitons in a realistic environment;
- a quasi-stationary approximation has been developed to efficiently model acoustic effects of the time-dependence of the environmental parameters. New and improved techniques have been put forward to incorporate data on oceanic currents into acoustic propagation models based on a coupled-mode representation of the field and a wide-angle, energy-conserving, 3-D parabolic approximation;
- recommendations have been made on reliability of predictions for various acoustic observables obtained assuming range-dependent ocean and disregarding horizontal refraction and effects due to ocean currents and time-dependence of the environmental parameters;
- a theoretical approach has been developed for calculation of the correlation function of the low-frequency sound scattered by internal waves. This allows one to calculate error covariance matrix of the acoustic field in 3D inhomogeneous environment;
- a method of source imaging based on calculation of scattering matrix has been developed which can be used for visualizing and quantifying uncertainty associated with unknown topographic features in the shallow sea;
- uncertainties in the travel time of a transient acoustic wave scattered at a rough surface have been quantified.



Scientific Results (1)



- Propagation of statistical moments of acoustic variables, when achievable, provides a very efficient alternative to Monte Carlo simulations when mapping environmental fluctuations into fluctuations of the acoustic field.
- Horizontal refraction decreases ray travel times and adiabatic mode phase. In shallow water, internal wave soliton-induced horizontal refraction can result in travel time biases $O(10\text{ms})$ at propagation ranges as small as 10 km. In deep water, at ranges about 1000 km horizontal refraction due to internal waves with the Garrett-Munk spectrum leads to acoustic travel times being $O(10\text{ms})$ less than in 2D simulations.
- The magnitude of 3D acoustic effects associated with non-linear internal wave packets is very sensitive to the azimuthal direction of sound propagation and drastically decreases from its maximum value when the acoustic track deviates from an internal wave front by $O(1^\circ)$.
- Experimental data indicate that correlation radius of the acoustic field in cross-range direction at ranges $O(4 \text{ Mm})$ is of the order of 500 m – 1000 m. These observations are successfully explained theoretically by internal wave-induced sound scattering.
- A full-wave theoretical description of the average acoustic field has been developed and applied to estimate the role of 3-D effects at low frequencies.



Scientific Results (2)



- Small-scale surface roughness, which leads to multi-path propagation, always increases the average travel time of scattered waves as compared to travel time in the absence of roughness. Conversely, large-scale roughness, which does not change the number of specular points, typically results in a negative travel-time bias. For first arrivals, travel time bias is always negative and is controlled by the variance of surface slopes and elevations, respectively, for large and small-scale surface roughness.
- Different versions of the Garrett-Munk spectrum of internal waves, which are usually viewed as equivalent, result in drastically different values of environmental characteristics relevant to horizontal refraction of sound and, consequently, of predicted values of travel time bias and other acoustic quantities. WKB-type simplifications of the Garrett-Munk spectrum, which are implicit in many internal wave models and sound scattering theories, prove inadmissible for quantitative description of random horizontal refraction.
- Travel-time biases associated with sound refraction and scattering by unresolved inhomogeneities have important implications for various acoustic remote sensing techniques ranging from echosounding to ocean acoustic thermometry and tomography.